IDO-16806

QUARTERLY TECHNICAL REPORT
SPERT PROJECT
April, May, June, 1962

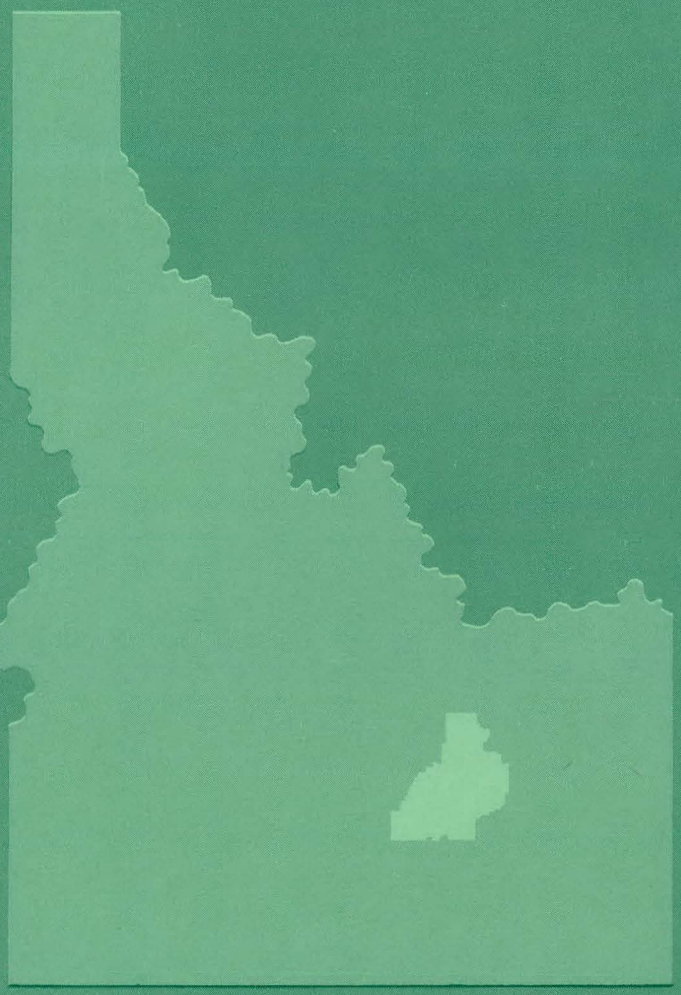

PHILLIPS PETROLEUM COMPANY

ATOMIC ENERGY DIVISION

NATIONAL REACTOR TESTING STATION
US ATOMIC ENERGY COMMISSION

DISCLAIMER

PRICE $1.00

Available from the
Office of Technical Services
U. S. Department of Commerce
Washington 25, D. C.

Printed in USA

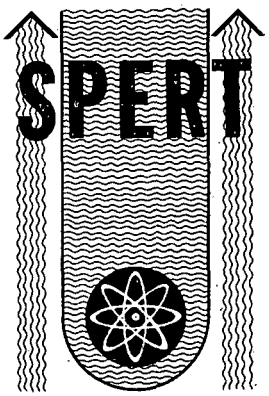

IDO-16806
AEC Research and Development Report
Reactor Technology
TID-4500 (17th Ed.)
Issued: September 21, 1962

QUARTERLY TECHNICAL REPORT
SPERT PROJECT
APRIL, MAY, JUNE, 1962

J. R. Huffman
Assistant Manager, Technical

W. E. Nyer
Manager, Reactor Projects Branch

F. Schroeder
Manager, Spert Project
Editor

PHILLIPS
PETROLEUM
COMPANY

Atomic Energy Division
Contract AT(10-1)-205
Idaho Operations Office
U. S. ATOMIC ENERGY COMMISSION

Previous Quarterly Reports
Spert Project

Quarter	IDO No.
1957	
3	IDO-16416
4	IDO-16437
1958	
1	IDO-16452
2	IDO-16489
3	IDO-16512
4	IDO-16537
1959	
1	IDO-16539
2	IDO-16584
3	IDO-16606
4	IDO-16616
1960	
1	IDO-16617
2	IDO-16640
3	IDO-16677
4	IDO-16687
1961	
1	IDO-16693
2	IDO-16716
3	IDO-16726
4	IDO-16750
1962	
1	IDO-16788

QUARTERLY TECHNICAL REPORT
SPERT PROJECT
APRIL, MAY, JUNE, 1962

SUMMARY

Static measurements of various nuclear core parameters were completed for the highly enriched plate-type aluminum-clad core to be used for the Spert I integral core destructive test program later this year. Self-limiting power excursion tests were performed with initial asymptotic reactor periods in the range of 934 to 4.6 msec in order to establish the transient response of the core and to obtain data for extrapolation to shorter-period tests in which violent destructive effects are expected. For tests with periods shorter than about 7 msec, fuel plate deformations were produced as a result of thermal stresses in the plates. Melting of fuel plates was obtained in two tests with periods of 5 and 4.6 msec. For tests with periods in the range of 9 to 4.6 msec, power burst shape changes have been observed which result in an increase in the ratio of the energy release in the total burst to that at the time of the power peak, as the period is shortened. Maximum transient pressures have not exceeded 10 psi for tests thus far performed.

A series of self-limiting power excursion tests has been initiated in Spert II to determine the effects of the initial system temperature on the kinetic response of the D_2O-moderated expanded core loading. The data indicate that as the initial system temperature is increased to near the saturation temperature, boiling becomes a more predominent shutdown mechanism with a consequent reduction in the peak power, burst energy, and fuel-plate surface-temperature rise observed. The increased dependence on steam formation for shutdown as subcooling is decreased does, however, lead to relatively larger amplitudes for power oscillations following the initial burst, apparently because of the larger unstable void volumes which are produced.

QUARTERLY TECHNICAL REPORT
SPERT PROJECT
APRIL, MAY, JUNE, 1962

CONTENTS

FIGURES

TABLES

I. SPERT I

1. INTRODUCTION

As was discussed in the previous quarterly report [1], a program of integral core destructive testing is planned for Spert I late in 1962. During the first quarter of 1962, a highly enriched, plate-type, aluminum-clad core (DU-12/25 core) was loaded in Spert I and a program of static measurements was initiated to determine various nuclear parameters of the core. This series of measurements was continued into April 1962 with a measurement of the flux profiles by cobalt wire activation and a power calibration of neutron level instrumentation.

Upon completion of the static program and preparation of instrumentation for transient testing, the transient testing program was initiated with a self-limiting excursion with an initial period of about 0.93 sec. This transient was the first of a fiducial series of transients intended to establish the basic transient properties of the DU-12/25 core and to obtain data for extrapolation into the short period region in which destructive effects are expected. The fiducial series included about 18 excursions with periods ranging down to about 7 msec at which point minor fuel plate deformations occurred. The observed deformations are thought to be the result of severe thermal stresses arising from nonuniform energy release within the fuel plates.

The testing program was then extended into the region of limited core damage. Four excursions were performed, each of which was initiated by successively larger reactivity insertions. Melting of fuel plates was observed in the last two tests which had periods of 5 and 4.6 msec. Severe widespread thermal deformation of fuel plates occurred in each of the four tests.

During the remaining two weeks of the 2nd quarter, detailed core inspections were performed, data analysis continued, and final preparations for the destructive test series were begun.

2. MEASUREMENTS OF STATIC NUCLEAR PARAMETERS

The measurement of various static nuclear parameters for the operational DU-12/25 core begun last quarter was continued to include calibration of the centrally located transient rod, determination of the neutron flux distribution, measurement of an isothermal temperature coefficient, and power calibration of the neutron level instruments.

The transient rod was inter-calibrated with the previously calibrated [1] control rods and the integral reactivity worth curve is shown in Figure 1. The total worth of the transient rod is $7.1.

Twenty-nine cobalt wires were inserted into the core in a distribution as shown in Figure 2 to obtain flux profiles during the power calibration experiment. The wires were irradiated at 95 kw for 135 min. Figures 3, 4, and 5 illustrate representative vertical flux profiles at selected core positions. The

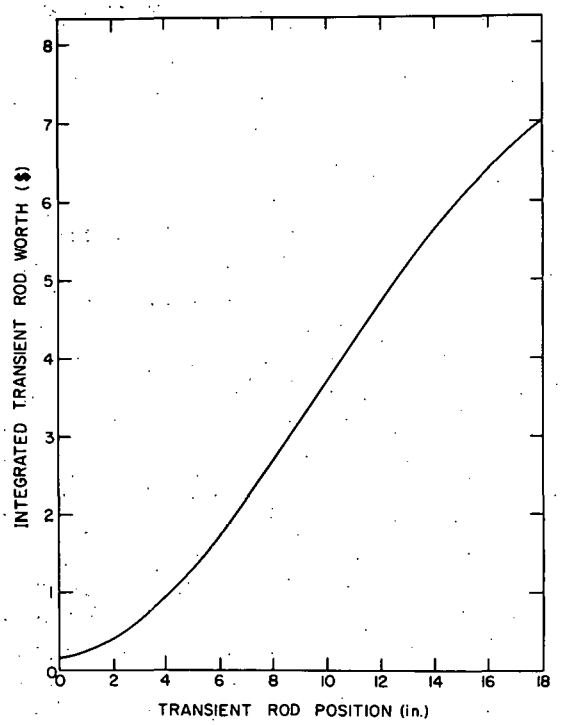

Fig. 1 Integral reactivity worth of transient rod.

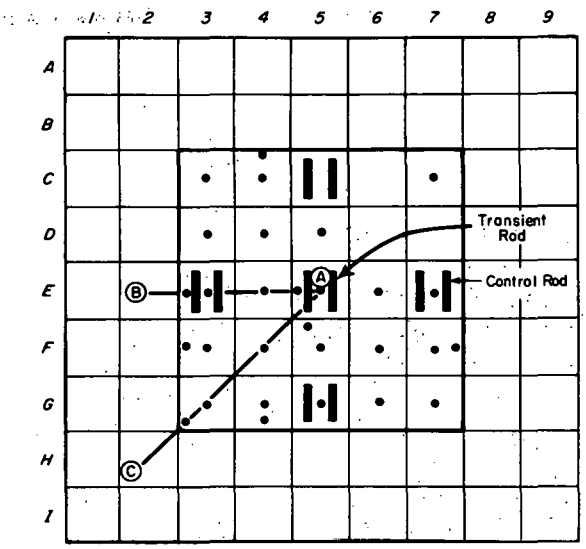

Fig. 2 Positions of cobalt wires for flux measurement activation.

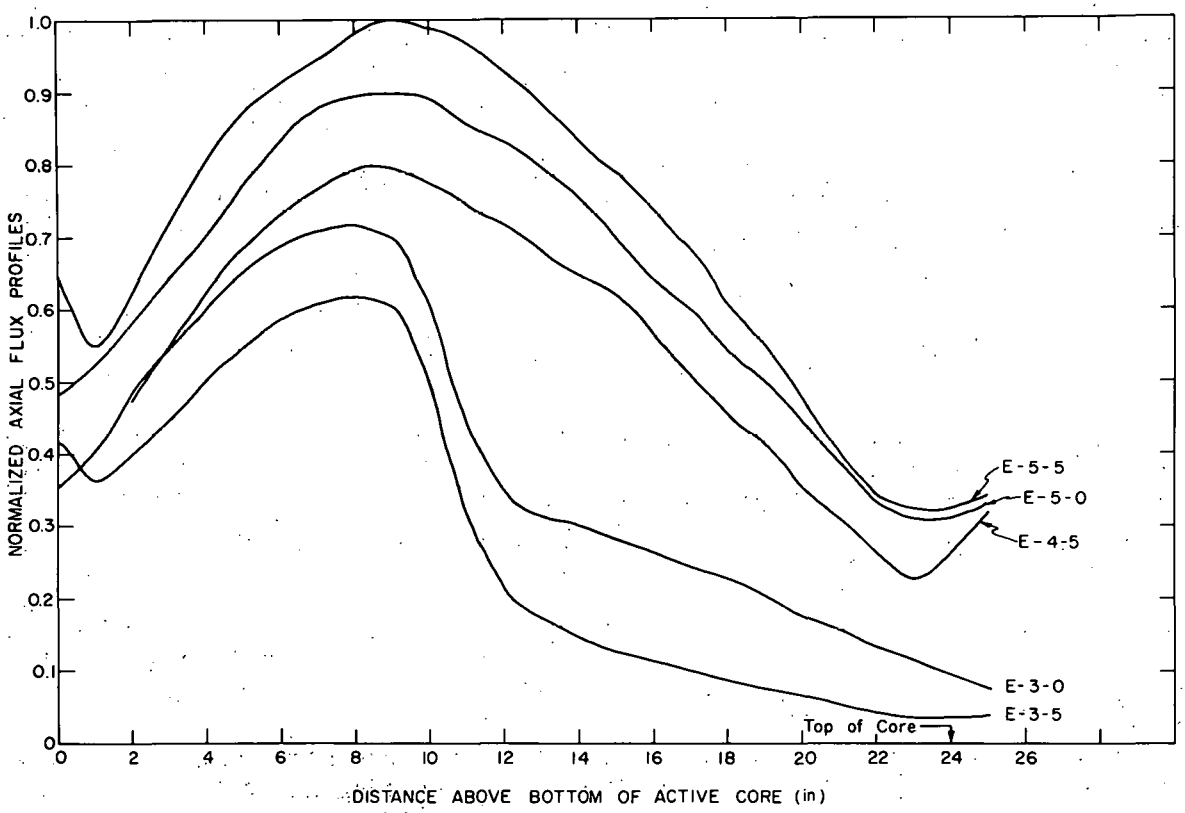

Fig. 3 Vertical flux profiles in fuel assemblies E-3, E-4, and E-5.

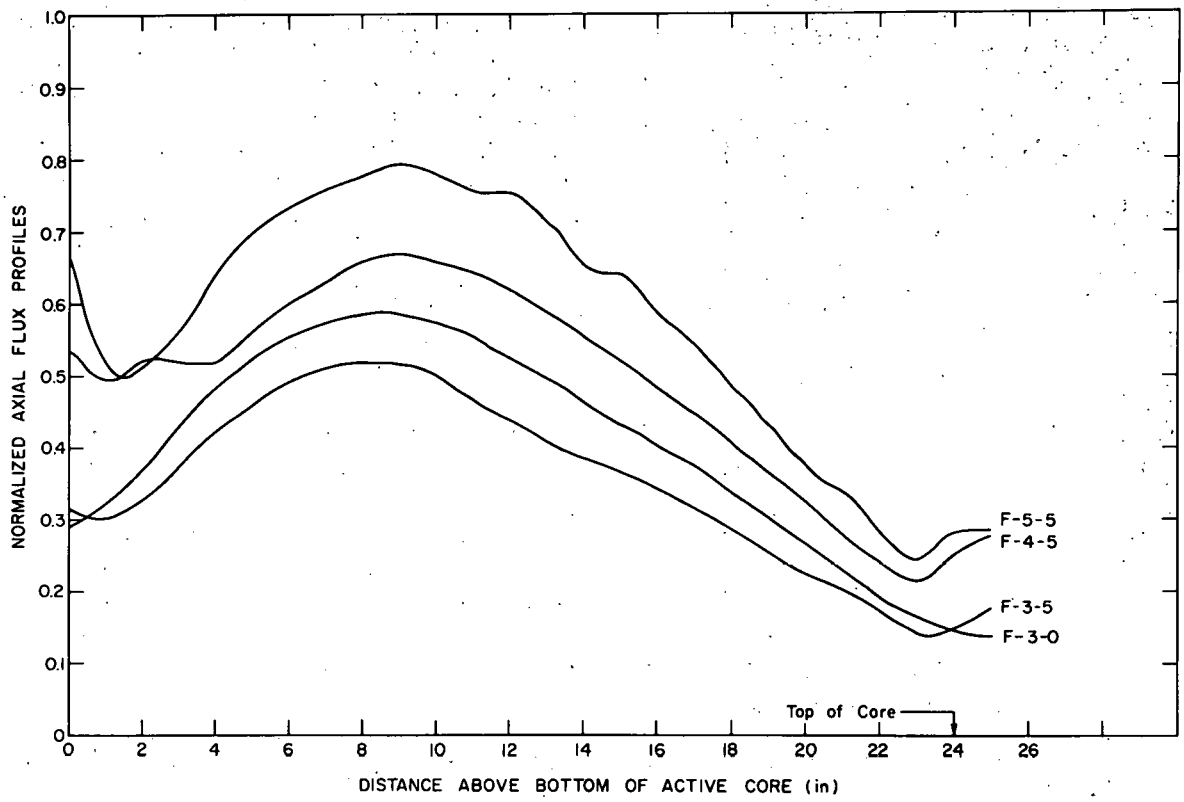

Fig. 4 Vertical flux profiles in fuel assemblies F-3, F-4, and F-5.

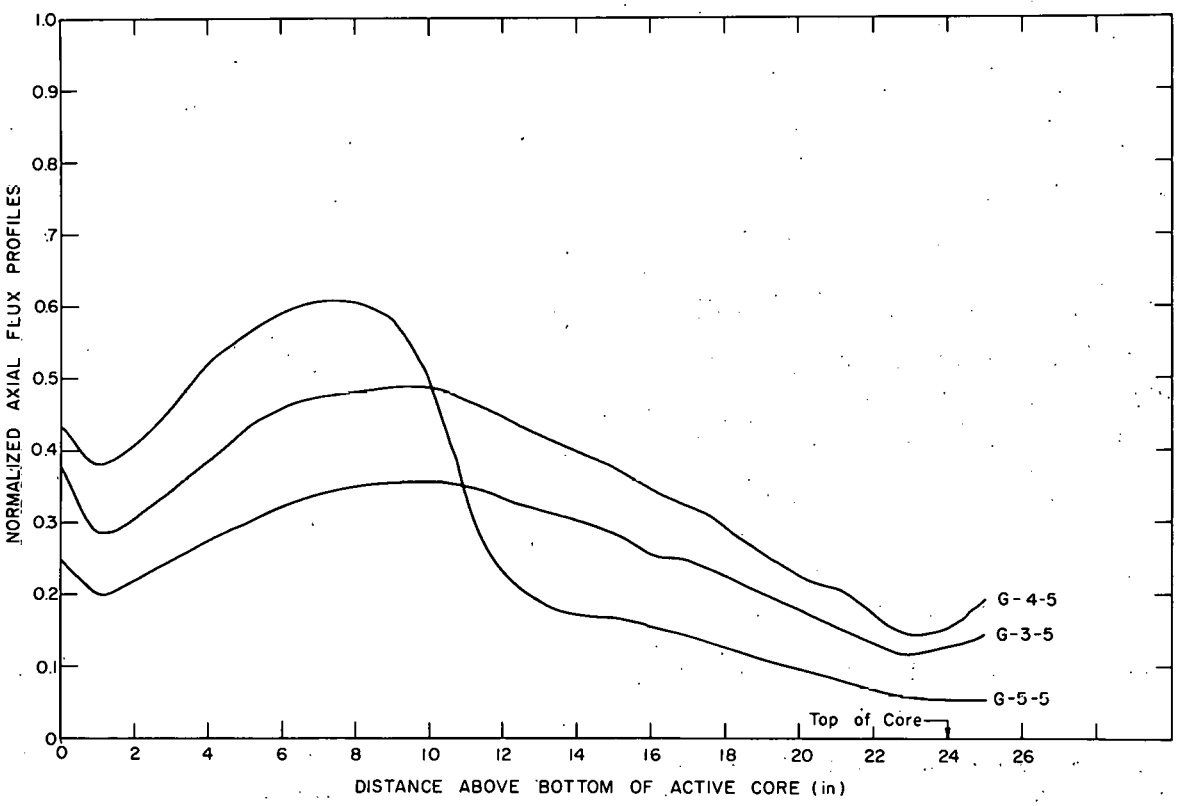

Fig. 5 Vertical flux profiles in fuel assemblies G-3, G-4, and G-5.

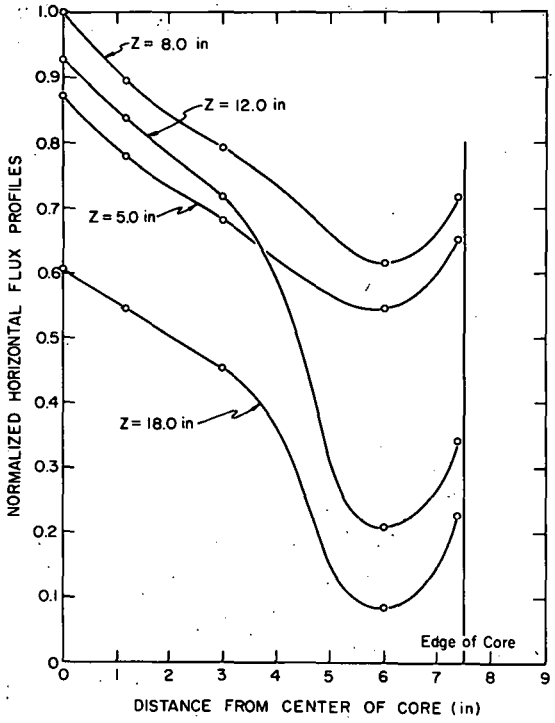

Fig. 6 Horizontal flux profiles along direction A-B (Fig. 2).

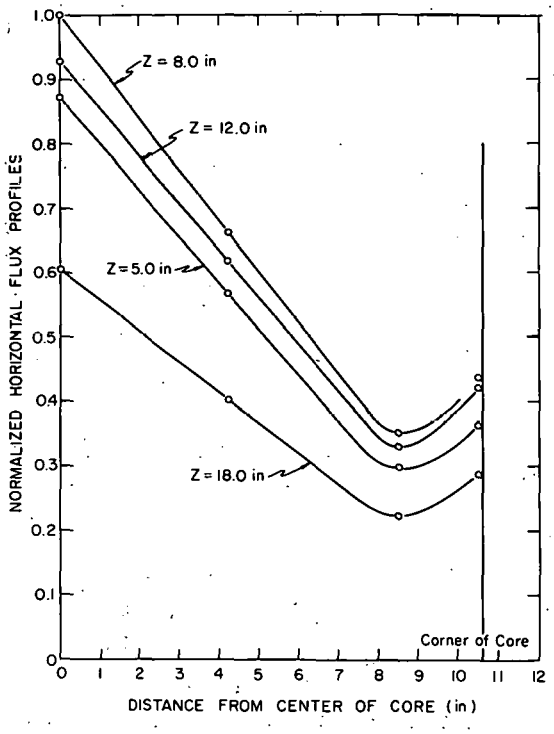

Fig. 7 Horizontal flux profiles along direction A-C (Fig. 2).

flux distributions are normalized to the maximum flux position which occurred about 8 in. above the bottom of the core in the central or E-5-5 position of the core. The designation E-5-5 indicates the fifth water channel (from left to right) of the E-5 fuel assembly (see Figure 2). Figures 6 and 7 present the horizontal flux profiles obtained along the lines A-B and A-C, respectively, shown in Figure 2, for various distances from the bottom of the core.

The relationship between chamber current and power level for several neutron-sensitive ion chambers was determined calorimetrically during this experiment. Figure 8 shows the approximate locations of the ion chambers relative to the core and the distances from the nearest core boundaries.

The isothermal temperature coefficient of approximately -2.1¢/°C was

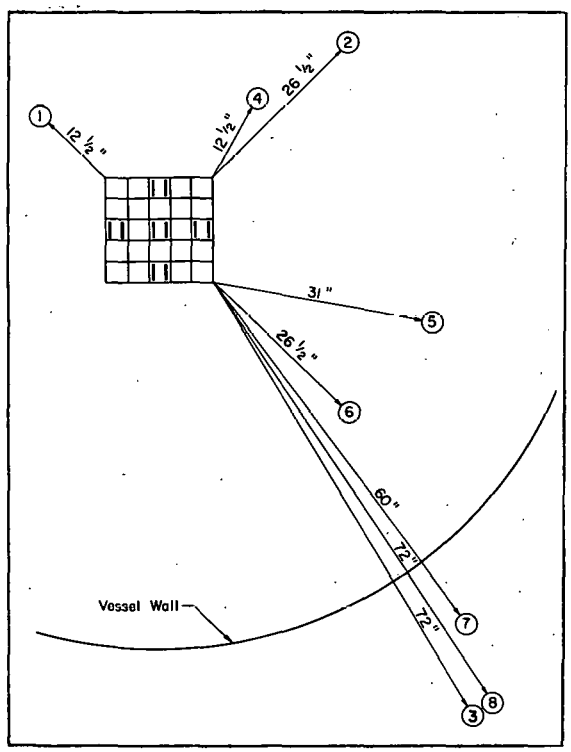

Fig. 8 Location of ion chambers.

determined from the change in control rod critical position during the 9.4°C temperature rise obtained during the power calibration.

3. TRANSIENT TESTING PROGRAM

A total of 32 self-limiting step transients was performed with the DU-12/25 core during the second quarter of 1962. Table I presents some of the results of these tests. In the table,

τ = the initial asymptotic reactor period

$\alpha = 1/\tau$

$\Phi(t_m)$ = peak reactor power

$E(t_m)$ = energy release at time of power peak

E_T = the total energy release in the burst

$\theta(t_m)$ = the maximum measured fuel plate surface temperature at the time of the power peak

$\theta(\max)$ = the maximum measured fuel plate surface temperature

Summary plots of these data are shown in Figures 9 through 12 where, for comparison, the results from three other aluminum-clad Spert cores also are shown. Peak power and maximum temperature data from the Borax I reactor also have been included.

As seen in Figure 9, the maximum power, $\Phi(t_m)$, attained in the DU-12/25 core is consistently lower than that for the other aluminum cores. Likewise, $E(t_m)$ is lower for this core than for the other cores (Figure 10). Both of these results were predicted and are explained in part by the smaller heat capacity of the DU-12/25 core. Since the reactivity compensating mechanisms for this core are dependent primarily upon temperature of core components and moderator, a given temperature rise will be achieved in this core with

TABLE I

TRANSIENT TEST DATA, DU-12/25 CORE

Date (1962)	Run No.	τ (msec)	α (sec^{-1})	$\phi(t_m)$ (Mw)	$E(t_m)$ (Mw-sec)	E_T (Mw-sec)	$\theta(t_m)$ (°C)	θ(max) (°C)
April								
5	1	934	1.07	0.67	1.84	(a)	65	89.4
10	2	642	1.56	0.98	1.76	(a)	66	94.8
10	3	357	2.80	1.5	1.47	(a)	60.1	98.5
10	4	163	6.14	3.25	1.13	(a)	58.5	105
11	5	98	10.2	6.6	1.34	(a)	69.1	110
11	6	65	15.4	14.2	1.68	(a)	92.2	115
11	7	47	21.3	27.3	2.25	3.95	110	117
11	8	34	29.4	55.7	3.22	5.46	121	124
12	9	25	40	86.7	3.21	4.91	130	132
12	10	19	53	141	4.07	6.04	144	149
12	11	14.5	69	210	4.10	5.83	156	165
12	12	12.1	83	318	4.44	6.68	165	180
12	13	10.2	98	415	5.23	7.57	183	226
13	14	9.5	105	445	5.91	8.15	188	256
16	15	8.2	122	565	6.21	9.10	185	318
17	16	7.2	139	740	6.53	9.80	164	377
17	17	6.9	145	802	6.45	10.4	183	404
19	18	6.8	147	842	6.80	10.6	189	382
19	19	6.4	156	860	7.12	11.3	186	460
May								
10	22	876	1.14	0.98	(b)	(a)	54	93
10	23	19.3	52	120	3.42	4.71	125	132
10	24	9.0	111	396	4.29	6.59	156	299
11	25	7.5	133	553	5.53	8.81	157	355
11	26	6.0	167	890	7.19	13.2	166	556
16	27	8.1	124	505	5.45	9.18	177	327
18	28	5.0	200	1130	8.34	17.5	295	675
June								
6	29	49.5	20.2	19.1	1.84	3.20	125	128
6	30	7.6	132	512	4.86	8.29	252	462
8	31	6.9	145	620	5.03	8.64	266	494
11	32	4.6	218	1430	8.74	19.7	332	683

(a) Total energy, E_T, undefined.

(b) Data not available.

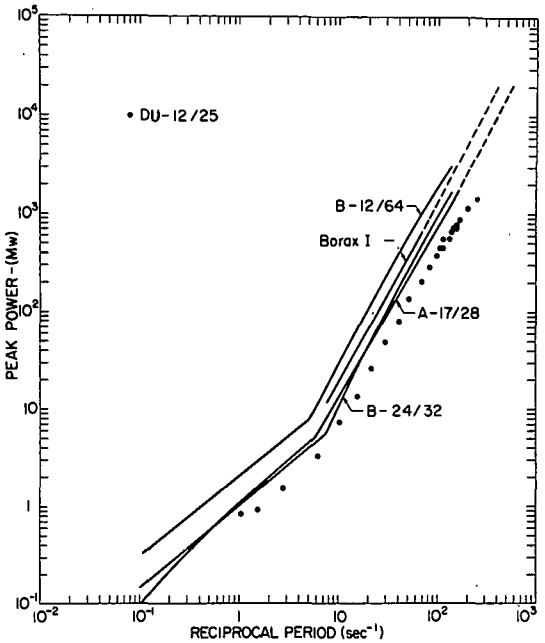

Fig. 9 Peak power as a function of reciprocal period for several aluminum plate-type cores.

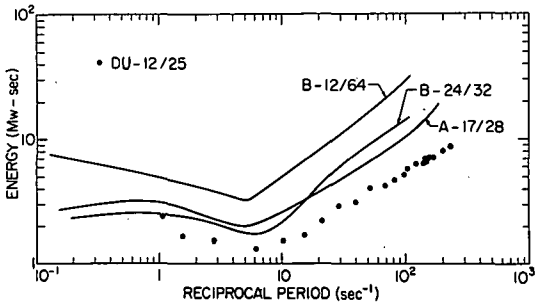

Fig. 10 Energy at the time of peak power as a function of reciprocal period for several aluminum plate-type cores.

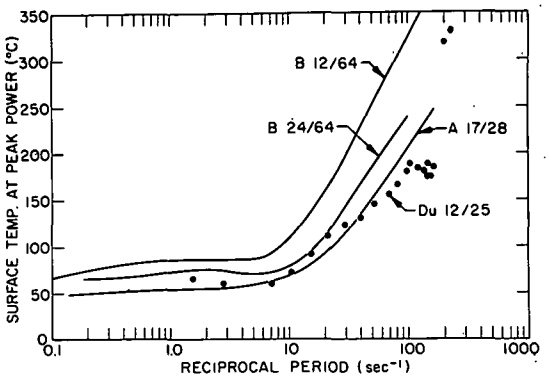

Fig. 11 Fuel plate surface temperature at time of peak power as a function of reciprocal period for several aluminum plate-type cores.

the release of less energy and consequently lower peak power.

It is noted that the shape of the curve defined by the power data points for the DU-12/25 core is, in general, similar to that for the other cores. In particular, it appears that the DU-12/25 peak power data are quite similar in trend to those of the A-17/28 core, but a factor of 1.5 times lower. Also, in the energy plots of Figure 10 it can be seen that the relationships between $E(t_m)$ for the various cores as a function of α are quite similar to the corresponding relationships between maximum powers, indicating that the power burst shape to time of peak power is nearly the same for all of these cores.

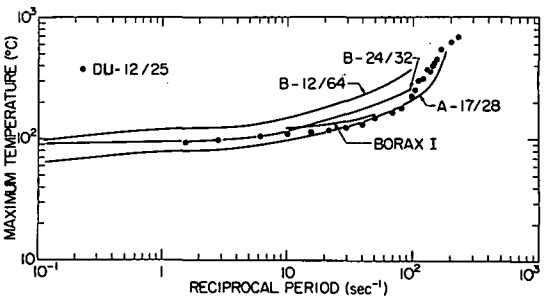

Fig. 12 Maximum surface temperature as a function of reciprocal period for several aluminum plate-type cores.

Even though $E(t_m)$ for the DU-12/25 core is considerably less than that observed for the B-24/32, B-16/32, and A-17/28 cores, the maximum measured fuel plate surface temperatures at time of peak power, $\theta(t_m)$, for these four cores are seen in Figure 11 to be nearly the same in the longer period region. The similarity of these data for several cores is, in part, to be expected as a result of the approximately equivalent void coefficient of reactivity, with the consequence that the temperature rise and void change would have to be approximately equal to provide a given reactivity compensation. The B-12/64 core, however, has a significantly lower density (or temperature) coefficient

of reactivity and consequently requires a larger temperature rise to provide the same reactivity effect.

The maximum measured fuel plate surface temperatures are shown in Figure 12 for the same aluminum cores. As can be seen, the data are nearly equal for all except the B-12/64 core, which, for the reasons stated above, attains higher values. The rapid rise in maximum temperature as period is decreased is thought to be a result of "vapor blanketing". With the attainment of temperatures much above 100°C, vapor blanketing can be established early in a power excursion, allowing the temperature to increase rapidly.

This behavior is demonstrated in Figure 13, in which the response of a typical thermocouple is shown in idealized form. A break from the initial exponential at t_2 usually occurs in the original data after several degrees of superheating. The decreased rate of temperature rise after t_2 implies a marked increase in heat transfer rate. At t_3, several milliseconds later, a temperature setback usually occurs followed by a rapid temperature rise. Experiments have shown that the setback is caused by an extremely high heat transfer rate as a massive volume of steam is suddenly generated on the fuel plate. After creation of this steam, heat transfer is greatly inhibited, as is reflected both in the rapid temperature rise during the remaining power burst, and in the relatively slow cooling rate after the burst. For shorter-period tests, boiling becomes less effective as a heat transfer mechanism. As a consequence, fuel plate temperature must rise more nearly in proportion to the total nuclear energy release. In the limiting case, energy release and temperature rise should become strictly proportional throughout most of the power excursion. Indication of this proportionality has already been seen in comparisons of temperature and energy for short-period transients. Referring again to Figure 12, the following regions may be defined:

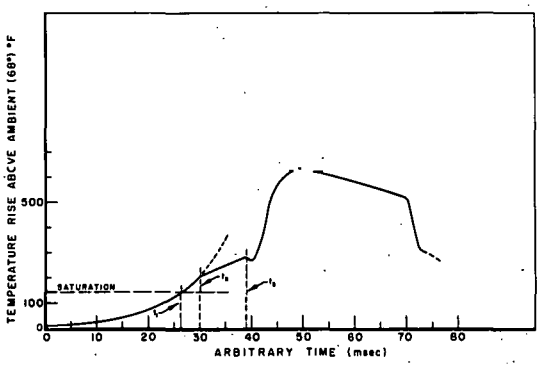

Fig. 13 Idealized fuel plate surface temperature behavior during a self-limiting power excursion.

Region I ($\alpha \lesssim 20$ sec^{-1})	Boiling heat transfer adequate to prevent appreciable superheat of plates. Maximum temperatures about 100°C.
Region II ($20 \lesssim \alpha \lesssim 100$ sec^{-1})	Transitional region. Occasional film blanketing reduces effectiveness of boiling heat transfer. Maximum surface temperatures begin to increase with α.
Region III ($\alpha > 100$ sec^{-1})	θ (max) primarily limited by E(total) with very little effect from boiling heat transfer.

In region I there exists a very weak dependence of θ(max) upon α since boiling is almost completely effective in preventing superheat. Region II, however, is characterized by a gradual increase in superheat and a complex dependence upon the conflicting roles of energy deposition and heat transfer. Finally, in region III, the maximum heat content in a fuel plate is nearly proportional to E(total).

As seen in Figure 10, $E(t_m)$ is a regular and predictable quantity. Experience with previous cores has shown that the total energy, E (total), in the region of $\alpha > 50$ sec^{-1} is also well-behaved with nearly the same dependence upon α and the ratio, R, of the total energy to the energy released to time of peak power has been nearly constant on several cores with a value of approximately 1.5. Tests performed on the DU-12/25 core have also demonstrated similar behavior for $50 \leqslant \alpha \leqslant 100$ sec^{-1}. However, for tests with periods below 10 msec, the ratio, R, has become much larger as indicated in Figure 14. It is clear that in this case the total energy as a function of α is increasing at a faster rate than the energy release at time of peak power. Since a constant value of R implies a constant power burst shape, the increasing value of R implies a change in burst shape as shorter periods are attained. In particular, there is a tendency in the DU-12/25 core to sustain high power levels following peak power. This has appeared as a "hump " on the backside of the power burst and can be seen in Figure 15, where several burst shapes have been normalized to a common maximum value and plotted in terms of time-in-periods.

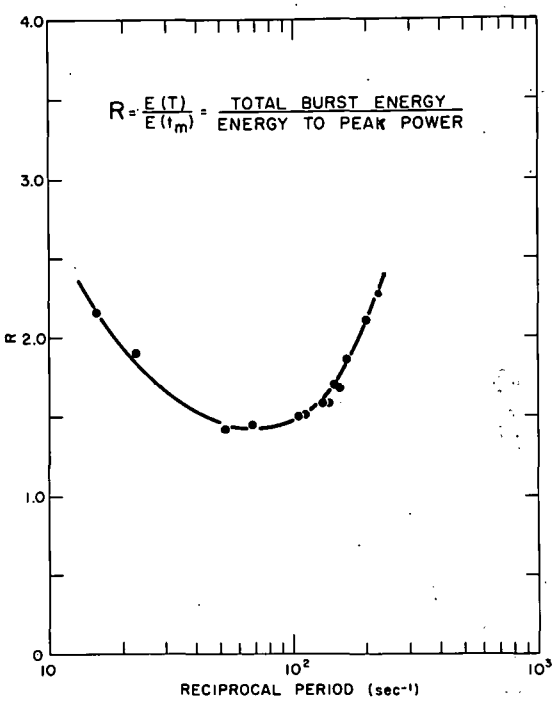

Fig. 14 Ratio of total burst energy to energy released at time of peak power as a function of reciprocal period.

The change in burst shape which is taking place with increasing α has several implications besides those of an increased energy release. Of more immediate interest is the apparent change in the time dependence of reactivity compensation. A change in reactivity at about the time of peak power is directly related to a change in slope of the log power, and it can be seen from Figure 15 that since post-peak curvature of the power trace decreases with decreasing period, the rate of production of shutdown reactivity is correspondingly reduced during this part of the excursion.

In Figure 15, a relatively constant burst shape is evidenced prior to peak power for the transients with periods from 9 to 5 msec. In the most recent test for which τ = 4.6 msec, however, a deviation from this behavior was observed. As the power approached maximum, an inflection occurred which resulted in delaying the power maximum several milliseconds from what would have been

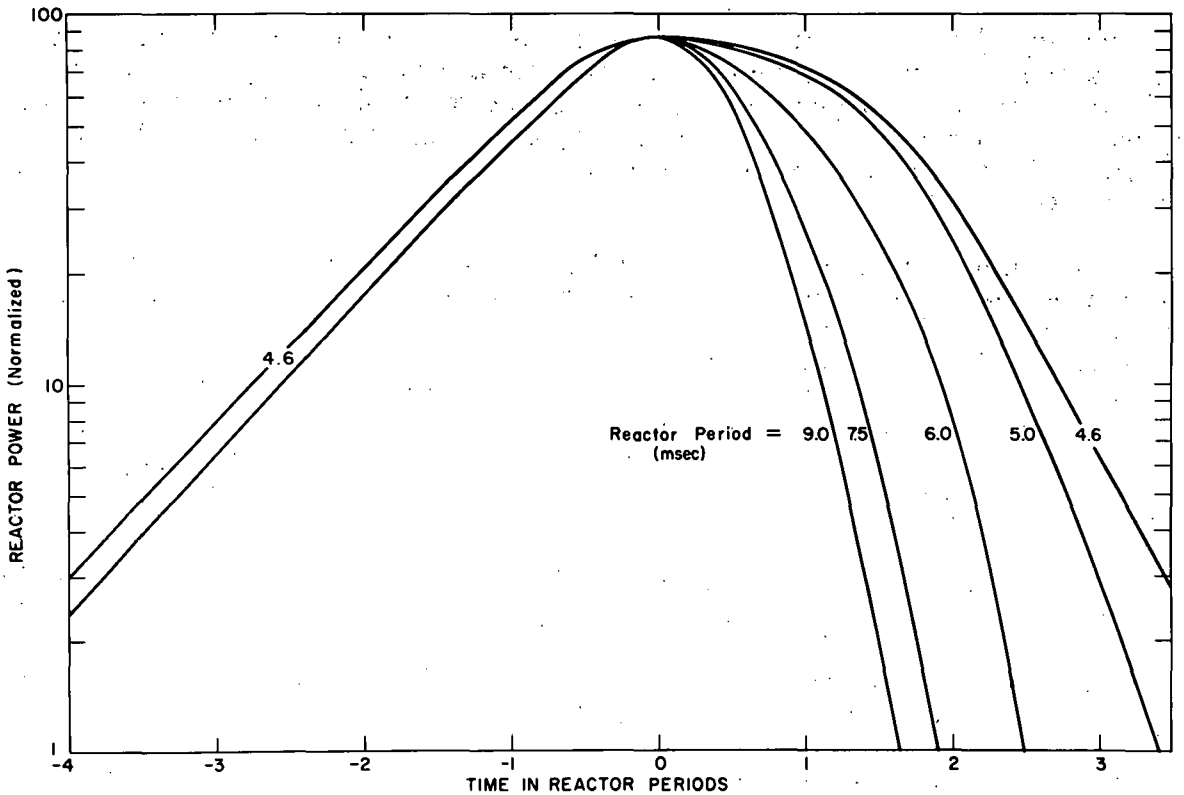

Fig. 15 Normalized power burst shapes plotted as a function of time in reactor periods.

predicted. In Figure 15, all plots are shifted on the time axis so that the time of peak power coincides and this shape change is clearly discernible.

Although burst-shape changes are easily seen in Figure 15, reactivity effects are more easily interpreted when the power is plotted as a function of real time as in Figure 16. Here, only magnitudes of the peak powers are normalized and time is in milliseconds, again shifted for coincidence of the power peaks. The post-peak curvature relationships are still in the same sequence as before, although less prominent. In the region of time just before peak power, curvature of the log power data is seen to increase as the period becomes smaller. Thus a situation exists before peak power which is just the converse of the post-peak behavior; that is, compensating reactivity is initially produced more rapidly as period is decreased. This is expected, since, with short-period excursions, both the amount of superheat and the fraction of the core experiencing superheat are increased.

Approximately 20 pressure transducers were installed in the Spert I reactor vessel. Figure 17 shows the three-dimensional array of pressure transducer positions about the core. Table II gives the coordinate of each position with respect to the core center and the maximum pressures which can be measured by transducers presently at each position. Since the very early rise of pressure, as well as maximum pressure, is of interest, it is necessary to use multiple installations at points of special importance (such as positions 3, 13, and 8) in order to obtain meaningful data throughout the dynamic range from a few psi up to several thousand psi. Pressures exceeding

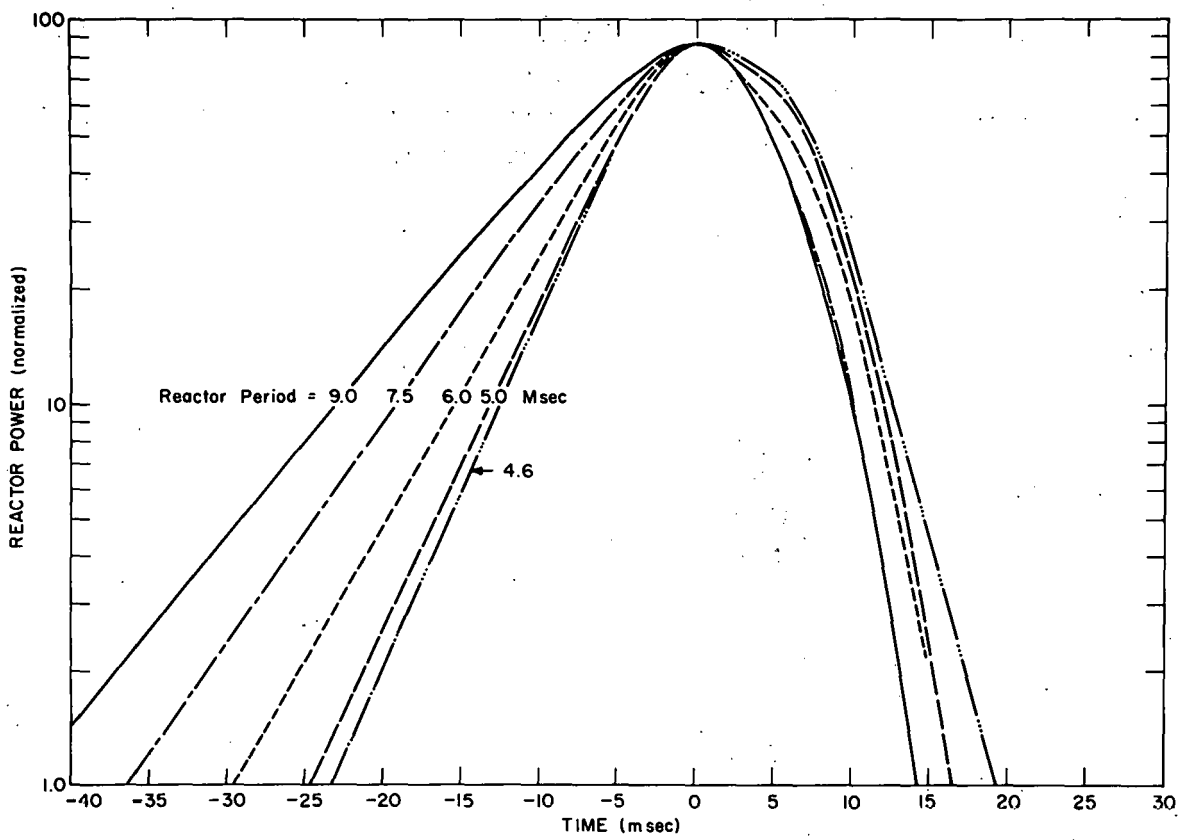

Fig. 16 Normalized power burst shapes plotted in real time.

10 psi have not been observed as yet, from this core; nevertheless, all ranges shown are recorded with each transient which has a shorter period than previously attained.

Measured values of the peak pressures observed for several of the indicated transducer locations are shown in Figure 18 as a function of the reciprocal period. Lines have been drawn to connect data points obtained from common position and do not represent any effort at fitting.

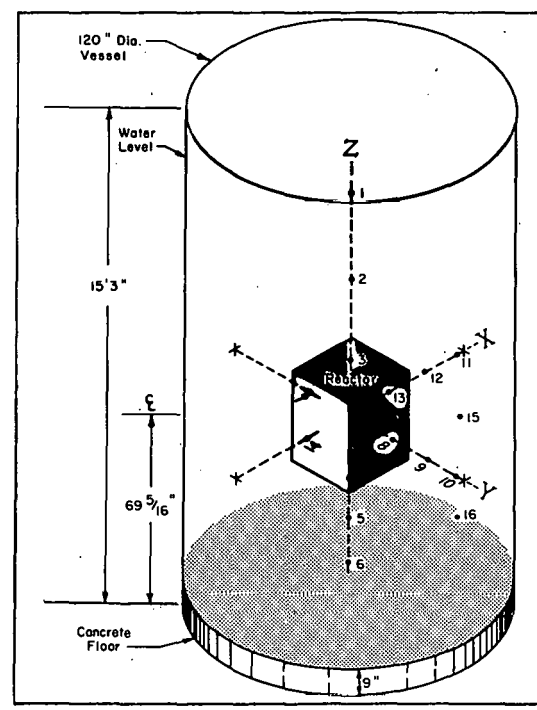

Fig. 17 Location of pressure transducers.

TABLE II

PRESSURE TRANSDUCER INSTRUMENTATION

Transducer	Coordinates (in. from core center) X	Y	Z	Pressure Ranges (psi)
1	2	3	58.5	100
2	2	3	40	1000
3	3	3	19.5	100, 300, 3000
4	3	3	-19.5	100, 3000
5	3	3	-40	20,000
6 (floor)	3	3	-52	300, 1000
7	0	-10.5	0	10,000
8	0	10.5	0	100, 300, 3000
9	0	25.5	0	1000
10 (wall)	0	55	0	300, 20,000
11 (wall)	52	0	0	300
12	25.5	0	0	10,000
13	10.5	0	0	100, 300, 3000
14	-10.5	0	0	1000
15	20	20	0	1000
16	20	20	-40	1000

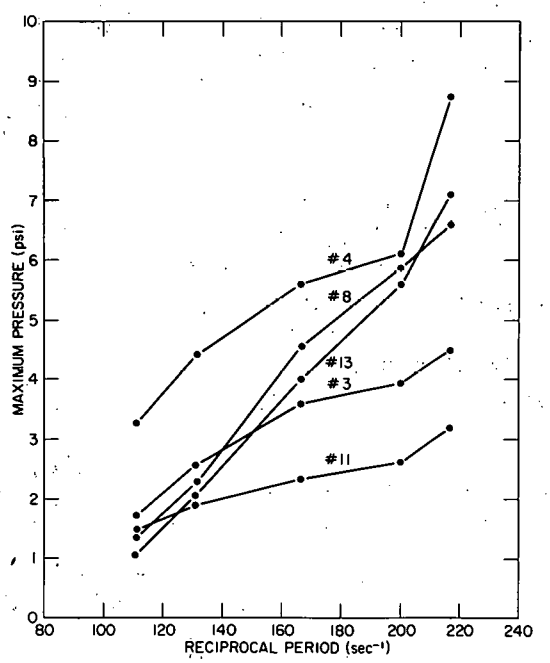

Fig. 18 Maximum transient pressure as a function of reciprocal period for 5 transducer positions (See Fig. 17).

4. DISCUSSION OF RESULTS FROM 5-MSEC-PERIOD TEST

Two of the power excursions in the test series conducted to date resulted in melting of fuel plates. These tests (Runs 28 and 32, Table I) yielded initial reactor periods of 5 msec and 4.6 msec respectively. For the 5-msec-period test melting was confined to portions of the six fuel plates in the central fuel assembly and one additional plate in an adjacent assembly. For the 4.6-msec test the region of melting was extended to include portions of plates from most of the nine central assemblies. Some results from the 5-msec-period test will be presented in this section. Data from the 4.6-msec period test will be presented in the next quarterly report.

Figure 19 presents the general nature of several measurements made during the 5-msec-period test and the temporal relationships to be discussed.

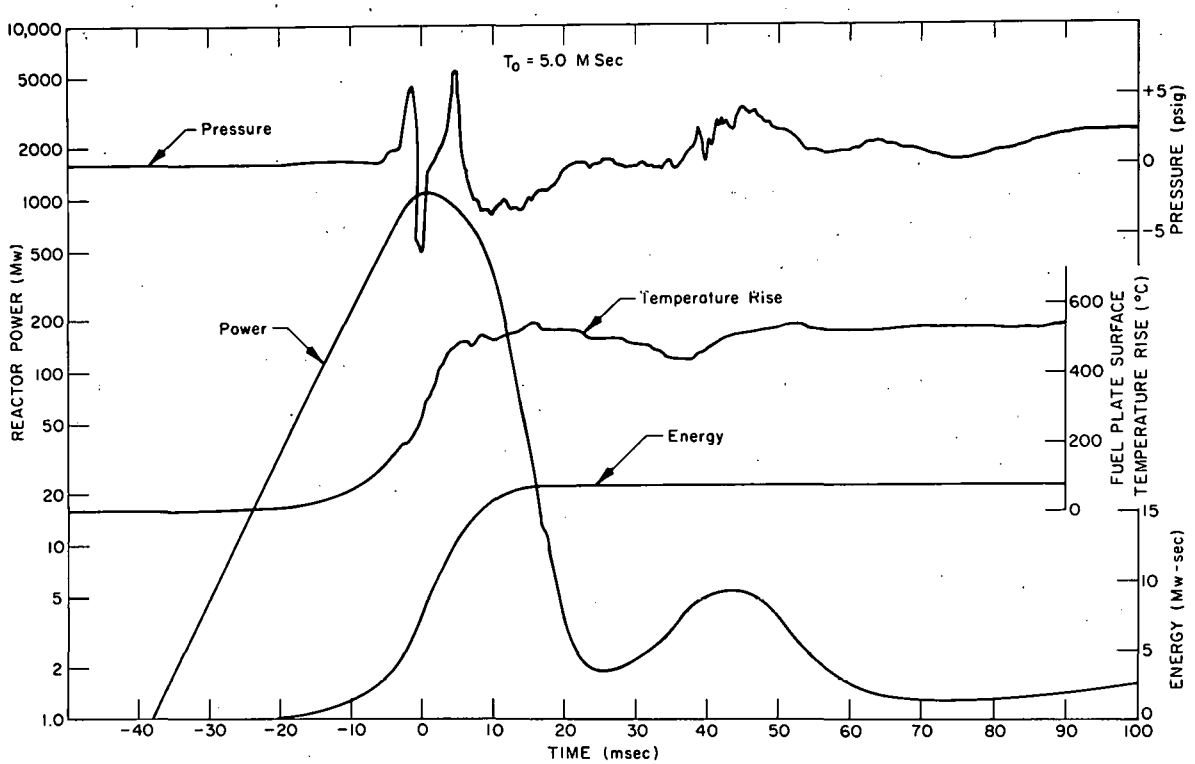

Fig. 19 Power, energy, fuel plate surface temperature, and pressure for 5.0-msec-period test.

Following the power peak and the post-peak "hump" discussed above, the power declines rapidly to an initial minimum of about 2 Mw, approximately 2.7 decades below peak power. A single oscillation is seen to occur about 43 msec after the initial peak and this is followed by a quasi-equilibrium power level of about 1.5 Mw for the duration of the test. The energy release and fuel plate surface temperature during this power burst show a behavior similar to that described above for longer-period tests. Examination of the temperature data indicates that the "break" from the initial exponential rise occurs at about 100°C temperature rise (initial temperature $\approx$ 15°C). This initial temperature break is not visible in Figure 19, but is apparent in the original oscillograph records and marks the time at which the initial phase of boiling first occurs.

Since the data shown in Figure 19 refer to approximately the hottest point in the core, this time ($t \approx -7$ msec) represents the first occurrence of boiling anywhere in the core.

A slight temperature drop can be seen to occur at about 200°C rise ($t \approx -3$ msec). By the time of peak power the boiling which causes this momentary temperature drop has probably blanketed the plate and, possibly, voided the entire water channel around the location of this thermocouple. Immediately following the temperature setback, a rapid temperature rise takes place at a rate approaching 60°C/msec. During this time, the plate is insulated from significant heat loss and the maximum temperature rise is thus indicative of the total energy release. The fluctuations measured in the surface temperature following the power peak are thought to be the result of instabilities in film blanketing, ie, momentary contacts of water with the fuel plate. In longer-period tests, the vapor blanketing has not been as complete and long-lasting as is evidenced here by the very long, sustained high temperature. Both partial and complete film breakdown are often indicated in the other temperature data shortly after peak power.

The transient pressure data shown in Figure 19 were obtained from a transducer located about 3 in. from the center of one side of the core (No. 13 as shown in Figure 17). Although all of the fuel plates in the DU-12/25 core are oriented normal to the Y axis shown in Figure 17, it has been observed that the pressure profiles measured on the X and Y axis are very similar. That is, the response from transducer 13, which is about 3 in. distant from the "X side" of the core and "looking" parallel to fuel plates, is almost identical in major details to the response of transducer 8 which is in a similar position on the Y side of the core looking normal to the fuel plates. Both "near-field" measurements display sharp pressure peaks just before and after peak power with a strong negative peak between, as shown in Figure 19. At greater distances from the core, as indicated by other transducers, the double peaks merge into a single, broad pressure pulse which is attenuated with distance.

All pressure transducers show a continuing oscillation after peak power with a 50-cps fundamental which appears to be the resonant frequency of the entire system (ie, water, tank, and steam). No counterpart of this oscillation is seen either in power or in fuel plate temperature data.

Initially, at about $t = -6$ msec, a rapid rise in pressure to about 2 psi is seen on the near-field monitors and, to a lesser extent, on more distant monitors. This pressure rise coincides very closely with the time at which initial-phase boiling arises within the core on the hottest fuel plates and is attributed, therefore, to this process. Another rise in pressure to about 6 psi occurs at $t = -3$ msec. This rise is coincident in time with the momentary temperature decrease previously mentioned and probably is associated with the water expulsion necessary to terminate the power rise.

For this 5-msec-period test, the melting was generally confined to a region about 6 in. high in the center of the core, and involved about one percent of the total fuel plate area of the core. Figures 20 and 21 show typical damaged fuel plates from the central fuel assembly. The plate shown in Figure 21 was instrumented with six surface-type thermocouples. Figure 22 shows a close-up view of melting around the thermocouple located 9 in. above the bottom of the plate. Square-topped ripples were prevalent on most of the affected plates

as shown in Figure 23. As seen in Figures 24 and 25, cladding failures occurred preferentially in the regions of greatest plate curvature. A large crack can be seen in Figure 26 and many smaller fractures can be observed in Figure 27. In some spots, melting extended completely through the plates as seen in Figure 28.

In addition to the visual inspection of the fuel plates, metallurgical examination is being performed on representative fuel plate sections to determine the extent of "hot cracking" of the cladding material and melting at grain boundaries. Several "dye-checks" were made on plates which had no obvious cladding failure, and some of the results obtained are shown in Figure 29. In these photographs the plates have been covered with a white "fix" coat and cladding failures show up as the dark regions. Closer examination reveals these dark areas to be composed of many small fractures, some of which penetrate to the fuel.

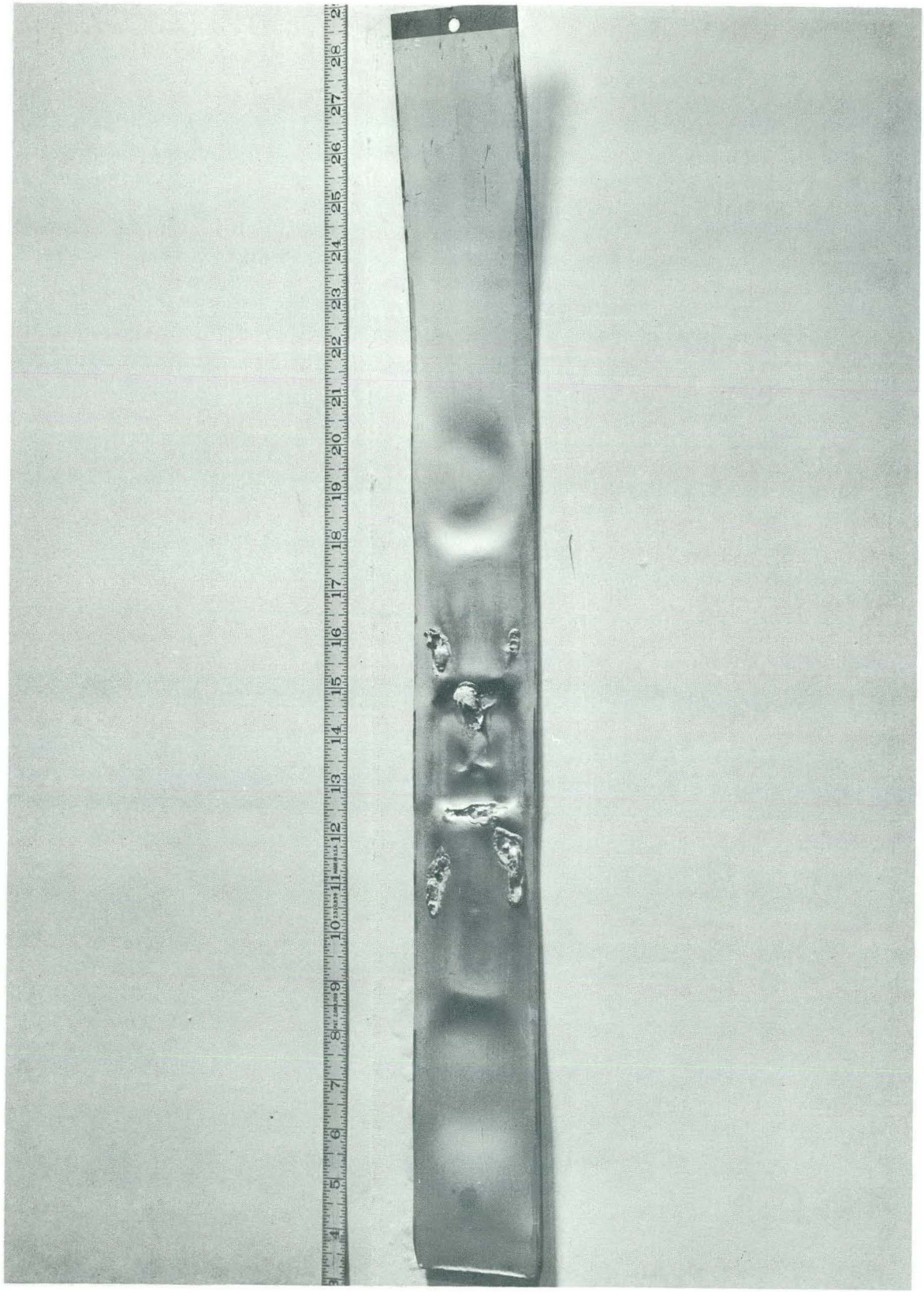

Fig. 20 Fuel plate damaged in 5-msec-period test.

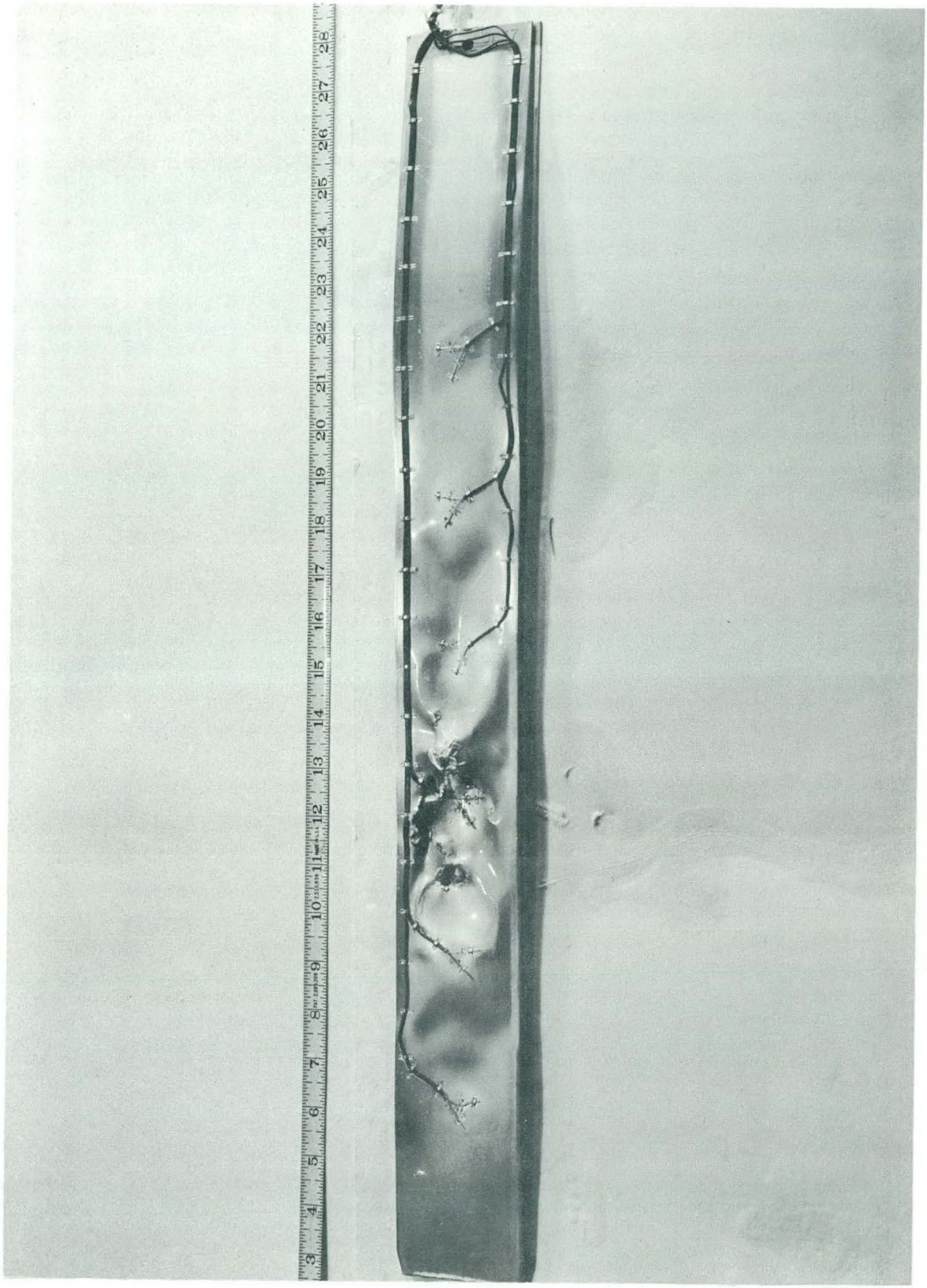

Fig. 21 Instrumented fuel plate damaged in 5-msec-period test.

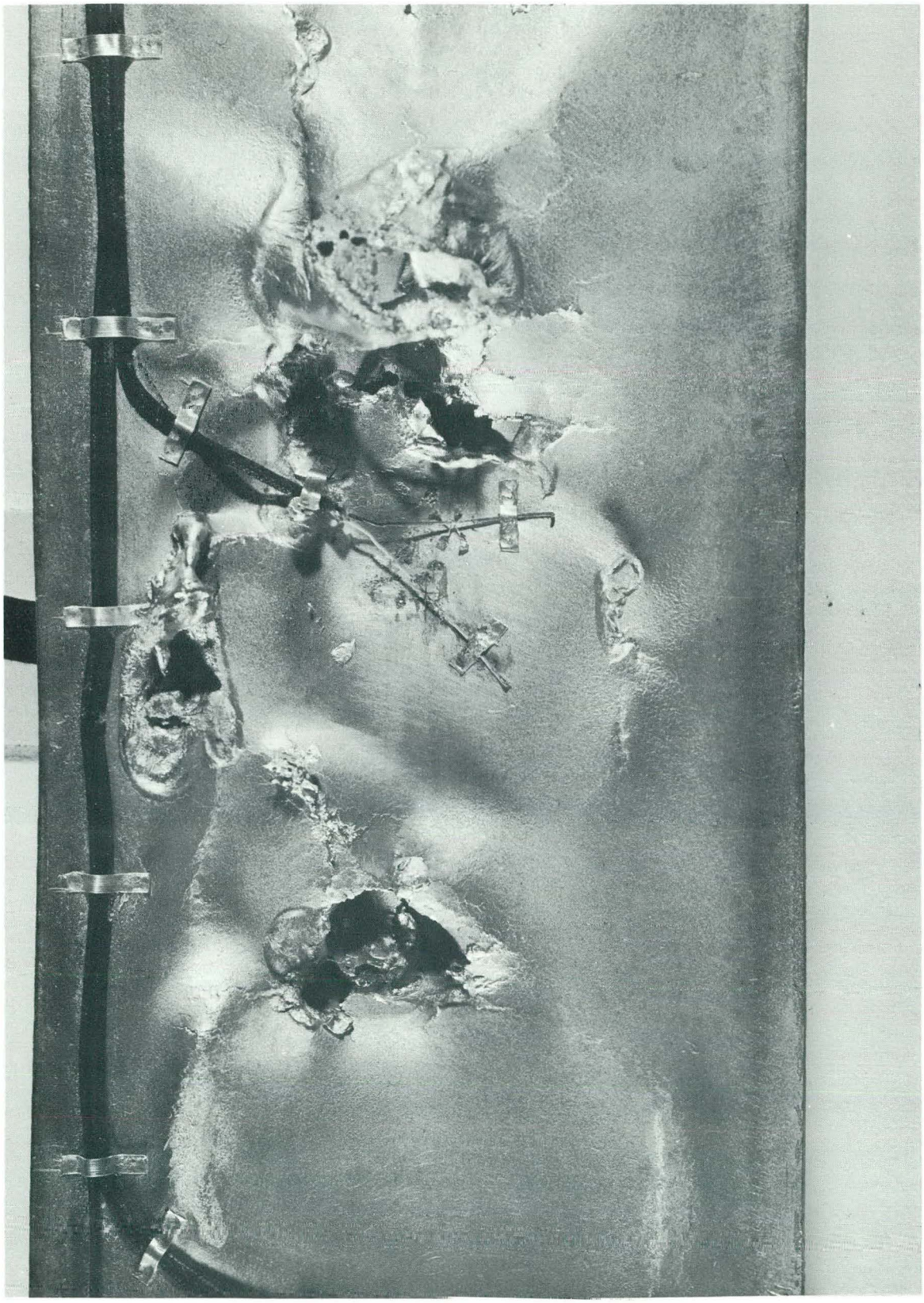

Fig. 22 Close-up view of thermocouple and melting shown in Fig. 21.

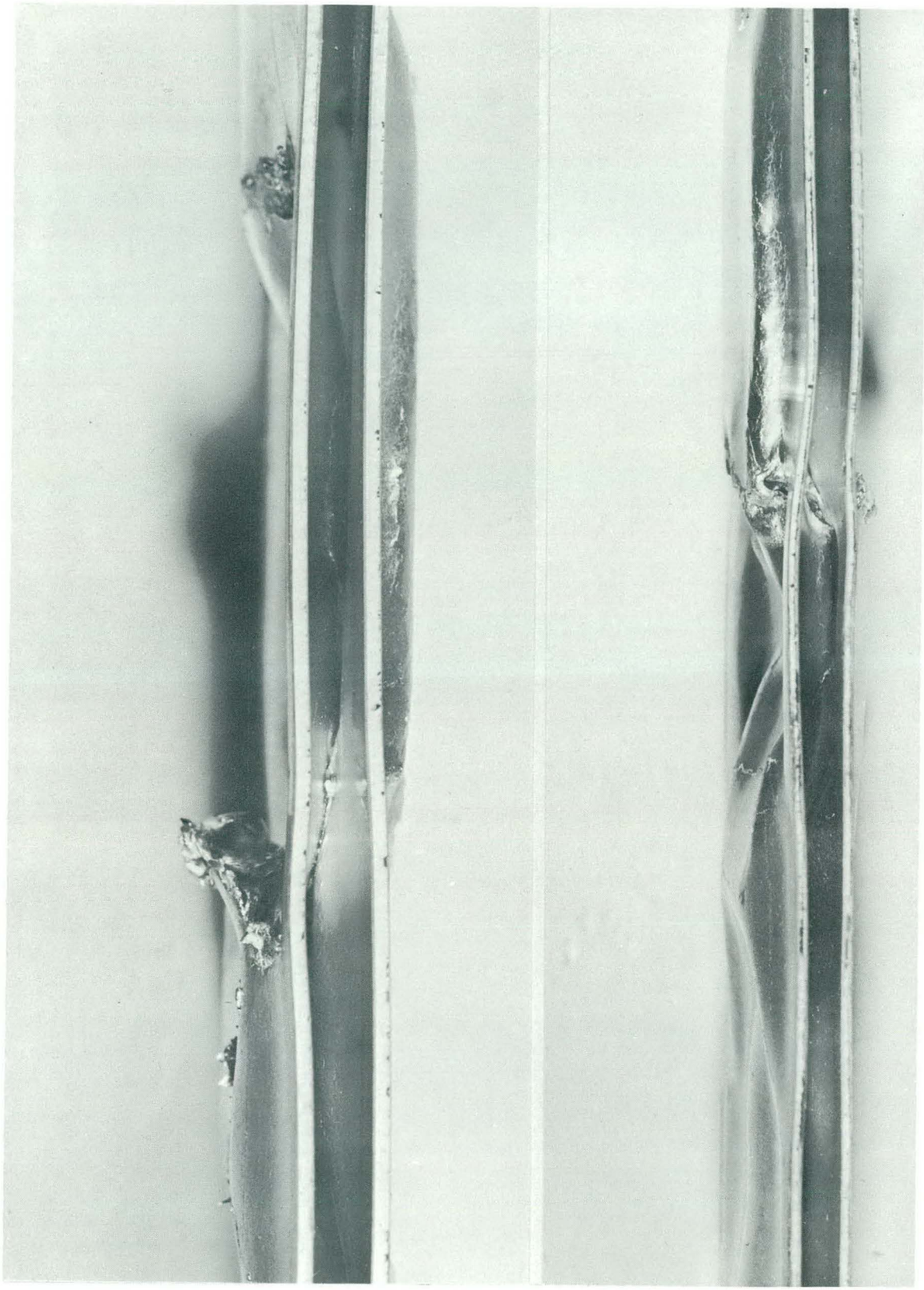

Fig. 23 Edge views of fused plates (5-msec-period test).

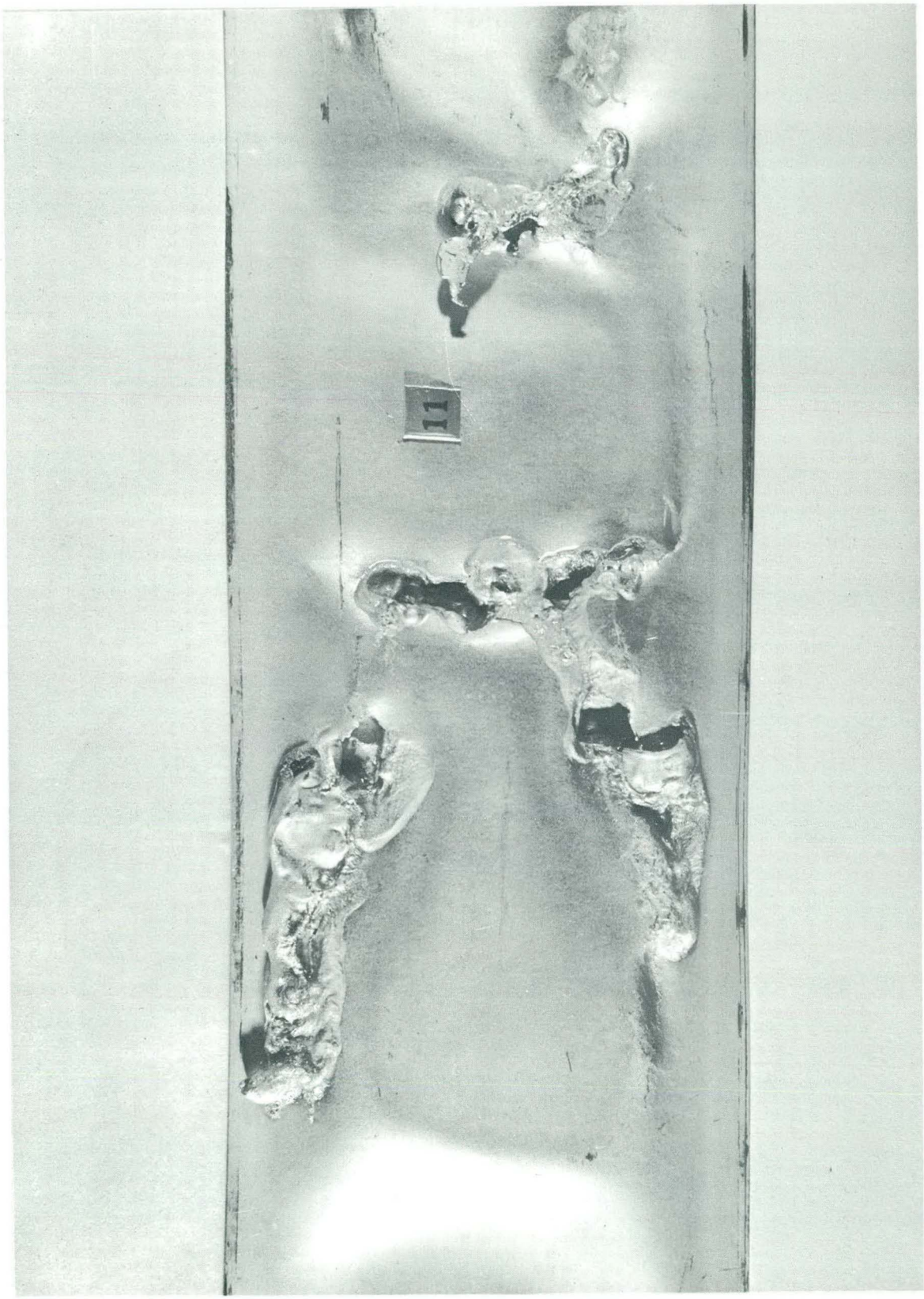

Fig. 24 Typical melt pattern obtained in 5-msec-period test.

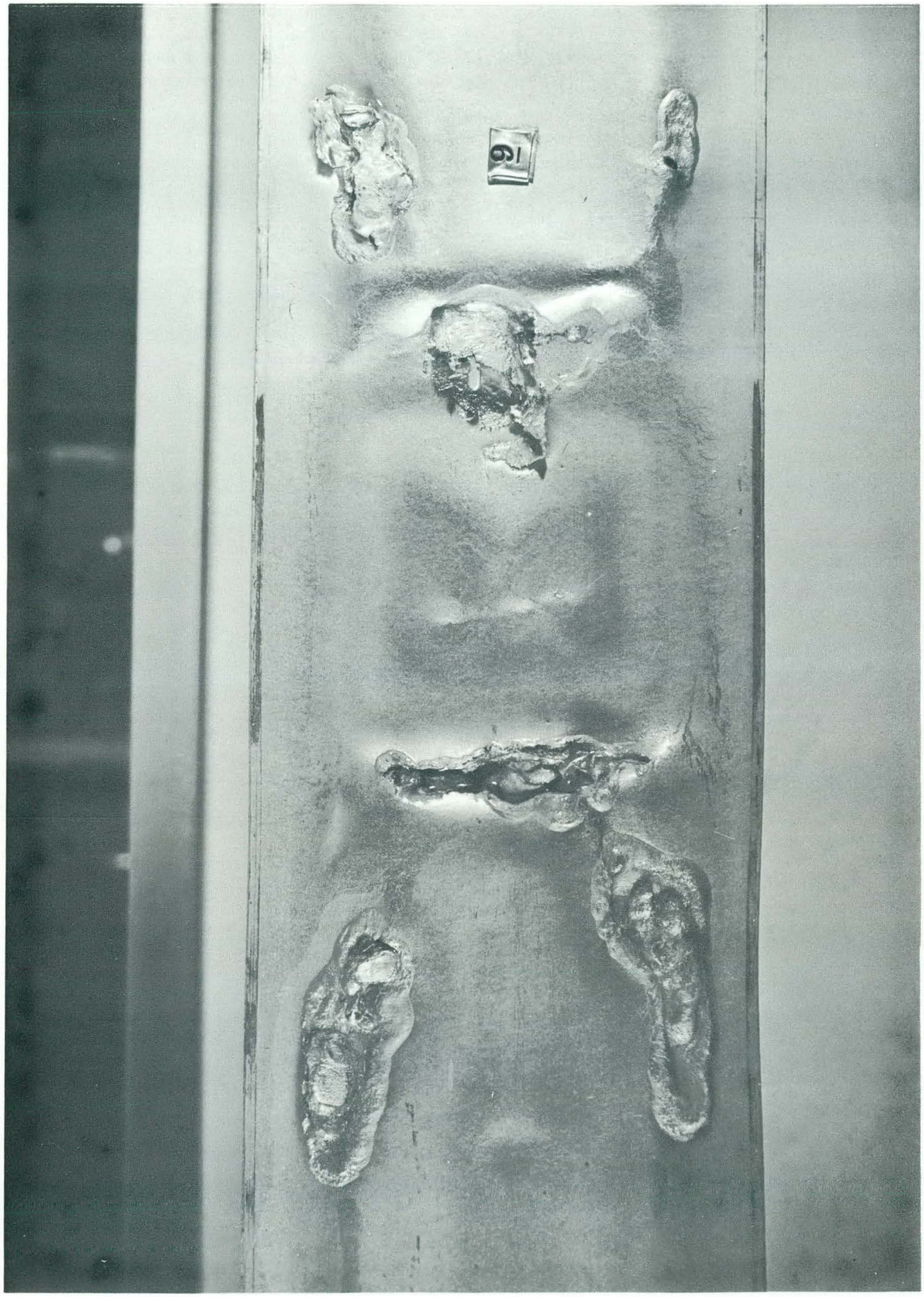

Fig. 25 Typical melt pattern obtained in 5-msec-period test.

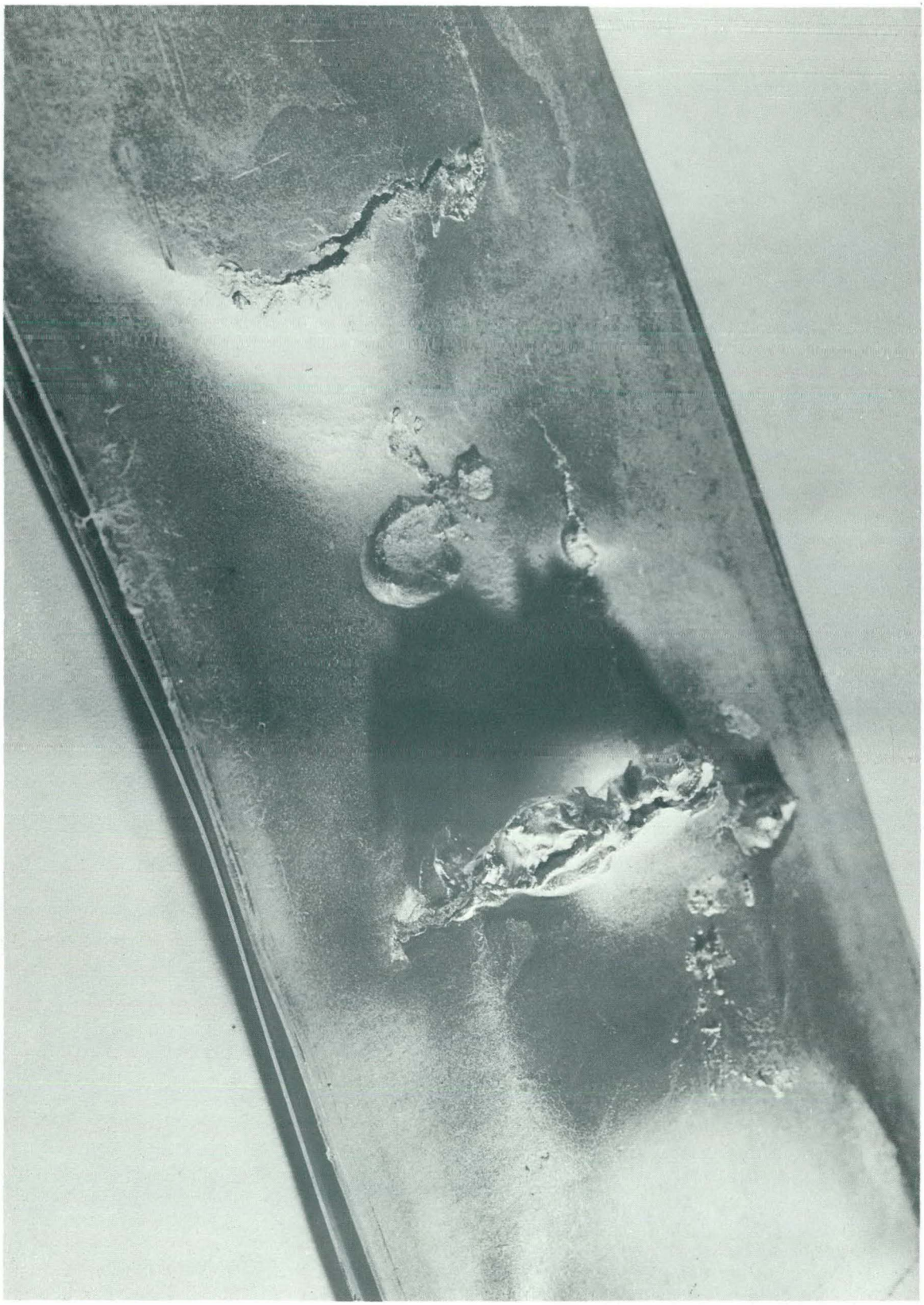

Fig. 26 Melts and fractures (5-msec-period test).

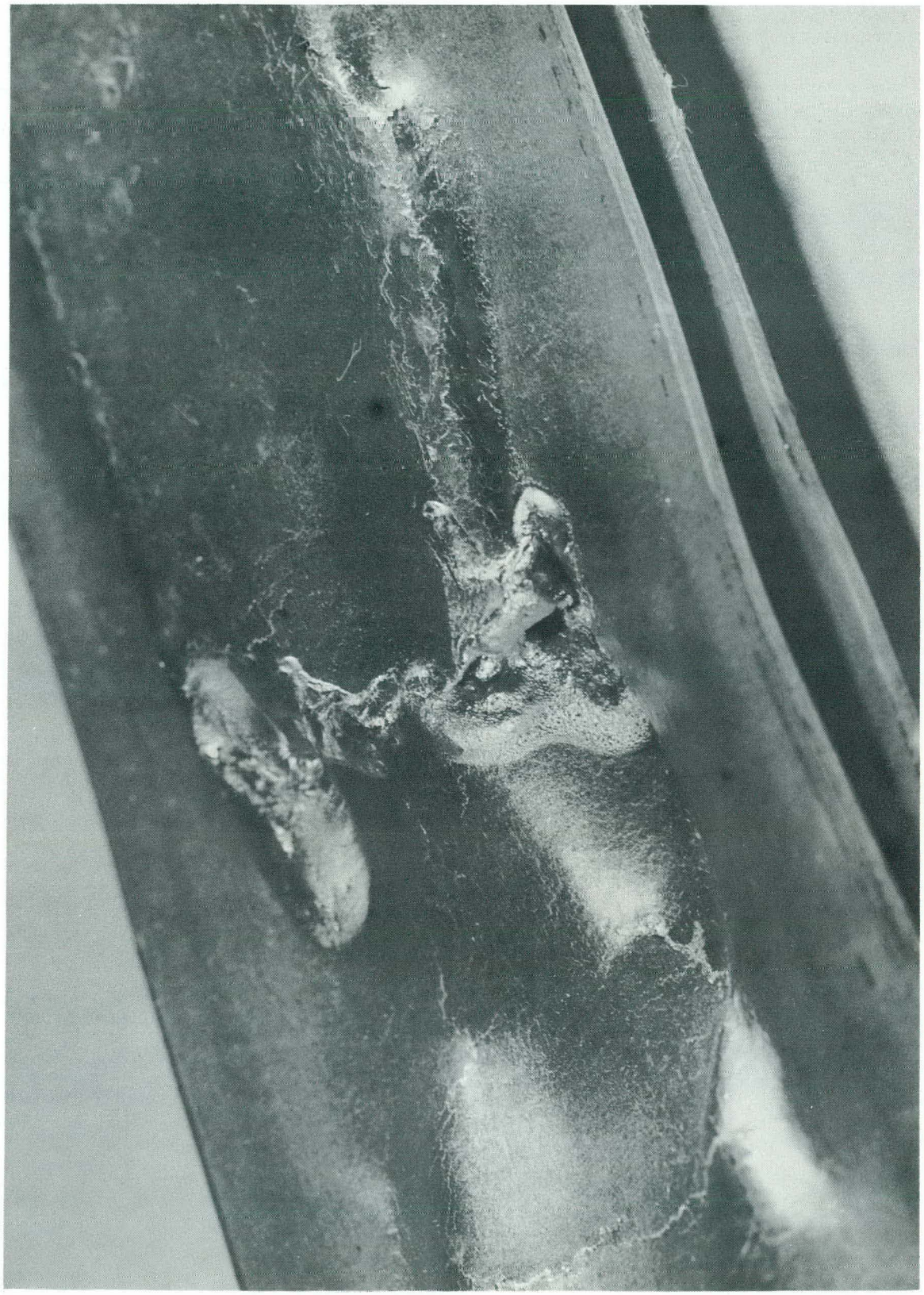

Fig. 27 Melts and fractures (5-msec-period test).

Fig. 28 Close-up view of melt showing hole through fuel plate (5-msec-period test).

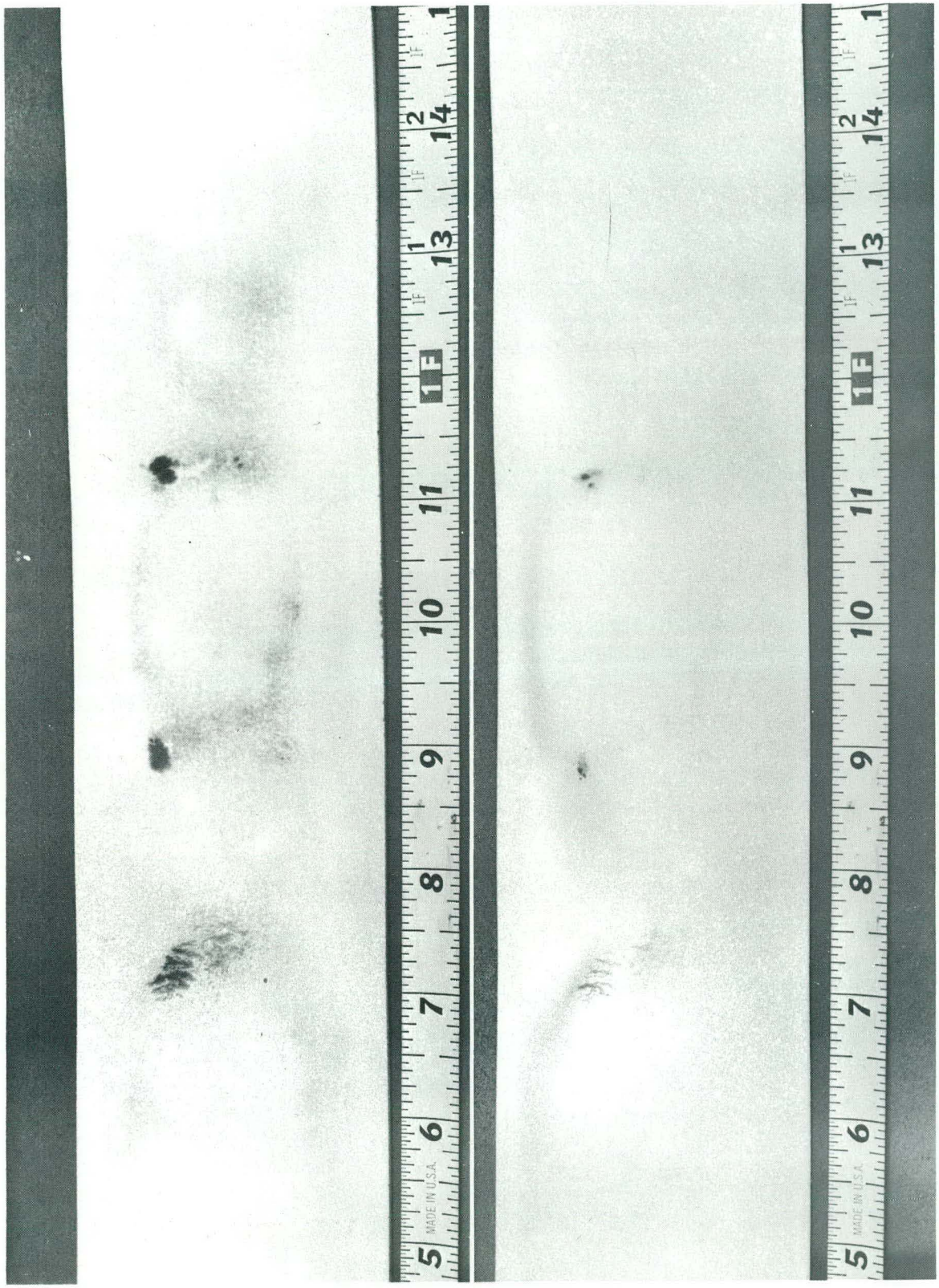

Fig. 29 Dye-check patterns on unmelted fuel plates. Dark areas indicate fracture (5-msec-period test).

II. SPERT II

1. EFFECT OF INITIAL SYSTEM TEMPERATURE ON SELF-LIMITING POWER EXCURSIONS

A series of self-limiting power excursion tests has been initiated to determine the effects of the initial system temperature on the kinctic response of the expanded D_2O core [2, 3]. These tests are initiated by step insertions of reactivity, with the reactor vessel liquid-full, with no forced coolant flow, and with the system pressure near atmospheric. Tests were performed with initial system temperatures from ambient (≈20°C) to near the saturation temperature (≈100°C).

The purpose of this series of tests is to supplement the information obtained during previous test series at ambient temperature and at various system pressures [4, 5], and to determine the effect of system subcooling (the temperature difference between initial temperature and saturation temperature) on the dynamic behavior of the expanded core. The range of system subcooling encompassed in the present (atmospheric pressure) series of tests is from ≈ 80°C to ≈ 1°C. In the pressurized test series, the subcooling extended up to 203°C. It is expected that as the initial subcooling of the system is decreased, the contribution to self-shutdown from non-boiling mechanisms such as plate expansion or moderator heating will decrease because the required temperature rise to the threshold of boiling is reduced. It is also clear that if the non-boiling contribution to the self-shutdown is reduced, the contribution of boiling or steam formation to the self-shutdown must be increased. Consequently, since steam formation is providing more of the shutdown as the subcooling is decreased and boiling will provide more shutdown reactivity per unit energy release than will non-boiling, it is to be expected that quantities such as maximum power, energy release, and maximum fuel plate surface temperature would be reduced as the subcooling is decreased. The preliminary results obtained to date in this test series are in agreement with these expectations.

The present test series thus far has included a limited number of 100-msec-period tests at initial system subcoolings of 20, 40, 60, and 80°C. Figure 30 illustrates the power behavior as a function of time for four self-limiting power excursions with initial periods of ≈100 msec and initial system subcooling of approximately 80, 60, 40, and 20°C. As the subcooling is decreased, the onset of boiling is achieved earlier in the initial burst, and the maximum power of the initial power burst is decreased. As the subcooling is decreased and shutdown becomes more dependent on steam formation, the growth and collapse of bubbles after the initial power burst will cause larger changes in reactivity due to the increased steam void fraction in the core. Consequently, the relative magnitude of the observed power oscillations following the initial burst becomes larger as the subcooling is decreased.

The magnitude of the initial power burst for these ≈ 100-msec-period power excursions as a function of the system subcooling is shown in Figure 31. The decrease in the peak power as the initial subcooling is decreased is expected since the energy required to reach the threshold of boiling has been decreased and the total amount of reactivity compensation provided by steam is increased.

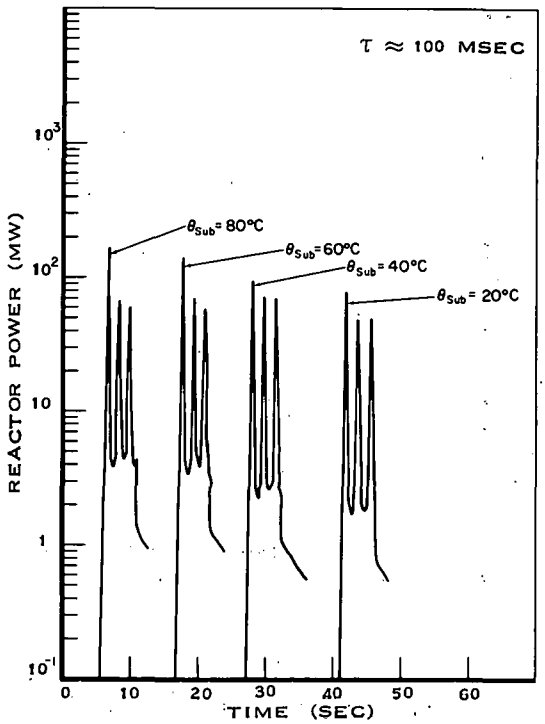

Fig. 30 Power behavior for 100-msec-period excursions at various subcoolings.

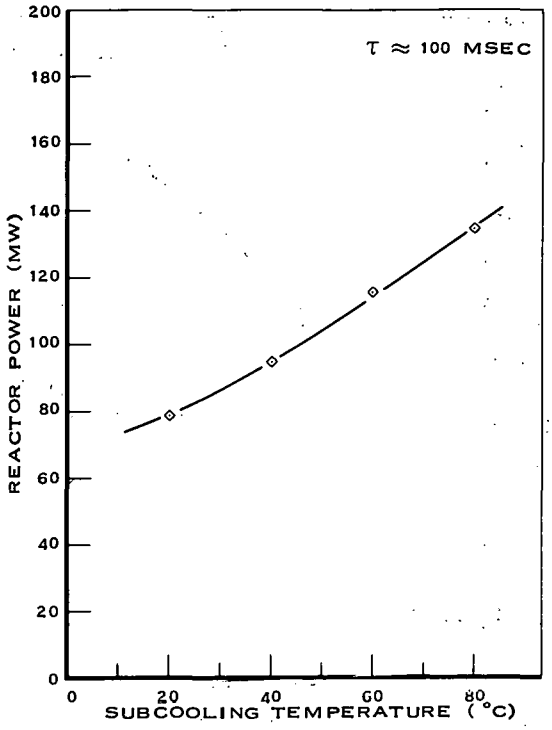

Fig. 31 Peak reactor power vs subcooling for 100-msec-period excursions.

This increase in steam formation provides more reactivity compensation for a given power or energy release than do the non-boiling mechanisms.

As can be seen in Figure 32, the temperature rise at time of maximum power for a representative fuel plate surface near the flux peak of the core is reduced by nearly a factor of two when the subcooling is decreased from 80°C to 20°C. The actual surface temperature reached at the time of peak power, however, remains relatively constant, decreasing slightly at higher system temperatures (lower subcooling). Thus for these tests in which boiling occurs prior to the power peak, the required reactivity compensation is apparently achieved primarily by boiling with a relatively constant value of fuel plate surface temperature required; that is, a relatively constant superheat above the saturation temperature. These limited data are in agreement with more extensive data for boiling shutdown obtained previously for Spert III [6].

The maximum temperature reached by the fuel plate surface after peak power is shown in Figure 33. This maximum temperature is more closely related to the energy release in the burst than is the temperature at the time of the power peak and hence, as expected, the maximum temperature decreases more markedly with decreased subcooling.

The data obtained in this test series indicate that as the initial system temperature is increased to near the saturation temperature, boiling becomes a more predominant shutdown mechanism. Since steam formation provides significantly more shutdown reactivity per unit of energy release than non-boiling shutdown mechanisms do, a reduction in subcooling permits earlier steam

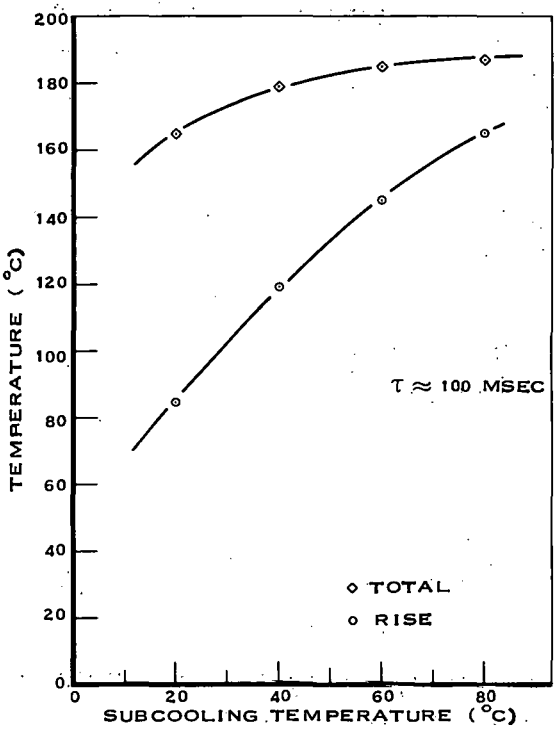

Fig. 32. Fuel plate surface temperature at time of power peak vs subcooling for 100-msec-period excursions.

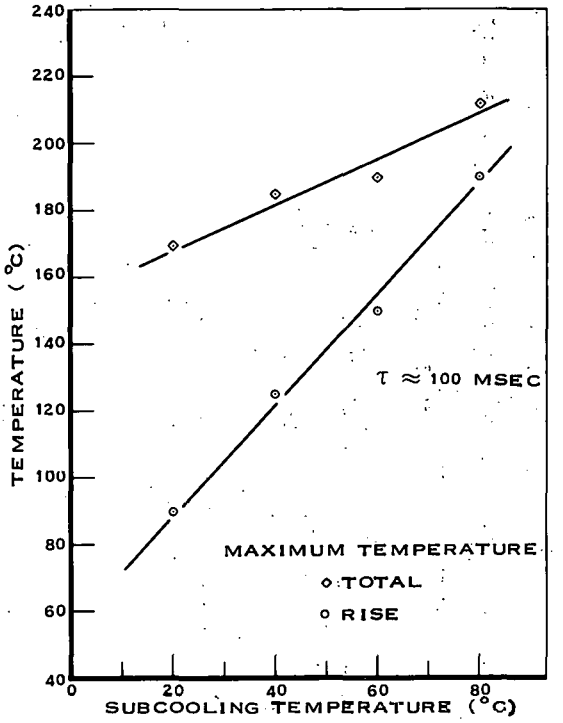

Fig. 33. Maximum fuel plate surface temperature vs subcooling for 100-msec-period excursions.

formation and earlier shutdown, with a consequent reduction in peak power, burst energy, surface temperature rise, etc. The increased dependence on steam formation for shutdown as subcooling is decreased appears to lead to relatively larger amplitudes for the power oscillations following the initial burst, apparently as a result of the larger unstable void volumes obtained with the decreased subcooling transients.

III. ANALYSIS

1. PROGRAM FOR PREDICTION OF SPERT IV INSTABILITY

An analytical program has been initiated to apply the ART-04 [8] and ART-03 computer programs to analysis of the forthcoming stability studies to be performed in the Spert IV reactor. (The ART-03 program is a frequency response program which is mentioned in Reference [7] and employs the method described in Reference [8].) With the exception of reactor parameter values to be obtained from the initial static experiments in Spert IV, preparation of the necessary input data has been completed.

The first application of the ART programs to the prediction of instabilities in Spert IV reactor will be to obtain the linearized feedback transfer function. This feedback transfer function can then be combined with the forward gain (zero power reactor transfer function), as determined from the neutron kinetic equations, to obtain the overall system transfer function. Examination of the changes in the overall system transfer function as a function of power level will provide a means for predicting the power level representing the threshold of instability for the reactor. A test of this method for predicting the threshold of instability for Spert plate-type reactors will be possible when experimental results have been obtained from the Spert IV stability tests.

2. LEAST SQUARES QUADRATIC SMOOTHING PROGRAM

A least squares quadratic smoothing program has been written for the IBM 650 computer. The objective was to develop a method by which digitized raw data can be smoothed without causing inaccuracies in the vicinity of an extremum (as in the case of the peak of a power excursion). The approach that had been used previously was to perform a least squares, straight-line fit. This linear program would allow a fit over an interval including as many as 100 data points, in order to determine a best fit near the center of the interval. However, when the line was fitted to a number of points sufficient to smooth the digitized data from a power burst trace, it was found in many cases that the peak value of the curve was lowered by an excessive amount.

The quadratic smoothing program will fit a quadratic form to as many as 49 data points in a given interval, and permits fitting to different numbers of data points in successive intervals. This flexibility permits the quadratic to be fitted to a large number of points in those regions in which the data are erratic (in order to achieve good smoothing) and to a small number of points near a peak (in order to avoid lowering the peak value). Such a change of the number of points fitted in various intervals will be necessary, however, only for cases in which the peak is extremely sharp and in which there are only a few data points in the vicinity of the peak.

The program will handle randomly spaced input data. The functional values of the smoothed curve at evenly spaced intervals are presented in the output. The size of the intervals for the output data may be specified.

Figure 34 is a plot showing the input points and the output points resulting from both the linear fitting and the quadratic fitting, for a set of input data points at randomly spaced intervals. The output points from the linear and quadratic smoothing programs are presented at 5-unit intervals. In both cases, fittings were made using 11 data points in each interval throughout the range, with no change in the number of points near the peak. It can be seen that the quadratic program provides a significantly better fit to the input data points.

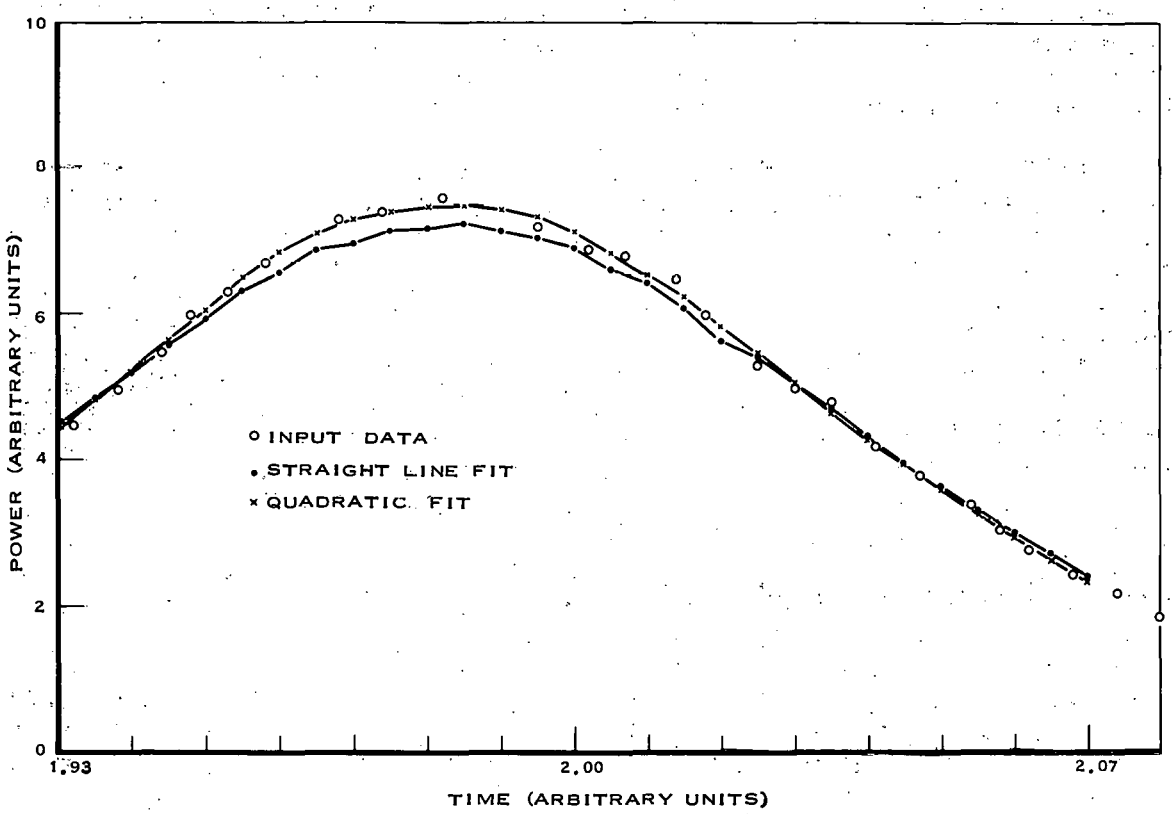

Fig. 34 Comparison of linear and quadratic curve fitting for typical power burst data.

IV. SPERT PUBLICATIONS ISSUED DURING THE SECOND QUARTER OF 1962

1. INTRODUCTION

This section presents a listing and short summary of the reports issued and the papers presented at national technical meetings by the Spert staff during the second quarter of 1962.

2. AEC REPORTS

(a) IDO-16762, Nuclear Startup of the Spert II Reactor With Heavy Water Moderator, J. E. Grund, T. H. Davis, and R. L. Johnson (Issued April 20, 1962).

A brief description is presented of the Spert II facility along with a description and the results of the static experiments with the initial D_2O-moderated core. The core is loaded with 3-in.- square, 24-in.-long, plate-type, highly enriched uranium-aluminum fuel assemblies on 6-in. centers. A core loading of 3.7 kg of U-235 has an available excess reactivity of approximately \$8.1 at 70°F and atmospheric pressure. The temperature coefficient of reactivity varies from about -2.0¢/°F at 80°F to about -4.4¢/°F at 300°F. The reactivity coefficients of temperature and void may be expressed as a density coefficient of -94¢/(percent density change) for uniform density changes or -7¢/(percent density change) when confined to the total water volume within the fuel assemblies. The reduced prompt neutron lifetime, ℓ/β_{eff}, was determined to be 0.11 sec.

(b) IDO-16773, Calculation and Measurement of the Transient Temperature in a Low Enrichment UO_2 Fuel Rod During Large Power Excursions, J. E. Houghtaling, T. M. Quigley, and A. H. Spano (Issued May 18, 1962).

This report presents the results of Spert I in-pile transient tests of a rod-type, low-enrichment UO_2 fuel element. The tests were performed to investigate the possibility of damage to such long thermal-time-constant fuel rods when subjected to short-period power excursions, and to test the effectiveness of an instrumentation technique for measurement of UO_2 fuel temperatures within the rods. In an initial series of power excursion tests, in which the range of reactor periods was from approximately 1 sec to 7.5 msec, simultaneous measurements were made of the transient temperature at the center of the fuel rod and at the outer cladding surface. Fuel rod rupture occurred during the exponential rise of the 7.5-msec excursion. Similar short-period tests performed on a second fuel rod containing no internal thermocouples did not result in cladding failure, supporting the postulation that rupture of the first rod was due to waterlogging of the UO_2 as a result of the cladding penetrations made for installation of the internal thermocouples. Calculations of the transient temperature distribution in the fuel rod have been made and the results are found to be in good agreement with the experimental data obtained on the central-UO_2 and cladding-surface transient temperatures.

(c) IDO-16774, Calculation of Departure from Nucleate Boiling Conditions for the Spert III Reactor in the High Pressure Region, J. Dugone (Issued April 18, 1962).

This report presents the calculations which were made to determine the safe steady-state power operating limits of the Spert III reactor from the viewpoint of fuel plate burn-out. A computer program was developed for the IBM 704 to aid in these calculations. The Bettis design departure from nucleate boiling (DNB) equation was used in conjunction with the LeTourneau and Grimble method of "hot channel" analysis in the development of the calculations. For cases where DNB occurs in the bulk boiling region, a modified Martinelli-Nelson two-phase flow correlation and some experimental single-phase pressure drop data were employed. DNB for a typical operating condition of 550°F inlet temperature and 2500 psig was computed to check the code. The results of the sample calculation show that at a steady-state power level of 60 Mw (maximum design power) the minimum flow rate required to prevent DNB is approximately 8000 gpm.

(d) IDO-16790, Spert I Destructive Test Program, Safety Analysis Report, A. H. Spano and R. W. Miller (Issued June 15, 1962).

This report reviews the objectives of the forthcoming Spert I destructive test program; the plans for the proposed program; the experimental results obtained to date, and extrapolation of these results to the destructive case; an analysis of the hazards involved in performing the destructive tests; and a detailed description of the reactor facility and environmental conditions.

3. PAPERS PRESENTED AT NATIONAL TECHNICAL MEETINGS

The following papers were presented at the annual meeting of the American Nuclear Society in Boston, June 18-21, 1962.

(a) "Shutdown Mechanisms and Reactor Safety", by W. E. Nyer, Trans. Am. Nuclear Soc., 5, 1, p 155 (1962).

This invited paper presented a review of the types of information presently being obtained on the nature of reactor shutdown mechanisms and served to introduce a session of contributed papers involving two topics of interest in considerations of reactor safety. The first, the physics of shutdown mechanisms, involved three sub-topics: the physical mechanisms by which shutdown effects are brought into play, the manifestation of these mechanisms as reactivity coefficients, and the way in which all of these factors enter into reactor plant behavior. The second main topic, the mathematics of shutdown mechanisms, was concerned with the calculation rather than the measurement of the physical effects, the coefficients and their interaction with the reactor.

(b) "Direct Measurement of the Dynamic Doppler Coefficient by Self-Limiting Power Excursion Tests", by A. H. Spano and W. K. Ergen*, Trans. Am. Nuclear Soc., 5, 1, p 157 (1962).

This paper described the direct, integral core measurement of the dynamic Doppler coefficient obtained from self-limiting power excursion tests performed with the Spert I oxide core [9].

(c) "Effects of Fuel-Rod Bowing During Self-Limiting Power Excursions in the Spert I Oxide Core", by W. K. Ergen* and A. H. Spano, Trans. Am. Nuclear Soc., 5, 1, p 172 (1962).

This paper presented experimental data and correlation of such data regarding the positive reactivity effects which were observed during a series of self-limiting power excursion tests of the Spert I oxide core and which were found to be related to bowing of the fuel rods caused by temperature differentials established across the rods during an excursion [9].

(d) "The Effects of System Pressure on Ambient Temperature Power Excursion Tests in a D_2O-Moderated Reactor", by R. L. Johnson and J. E. Grund, Trans. Am. Nuclear Soc., 5, 1, p 160 (1962).

This paper presented the results of tests performed in the Spert II reactor to investigate the effect of system pressure on the dynamic response of the D_2O-moderated core to step insertions of reactivity. Preliminary results of these tests were reported in a previous quarterly report [5].

(e) "High Power Reactor Describing Function", by A. A. Wasserman, Trans. Am. Nuclear Soc., 5, 1, p 165 (1962).

This paper presented the derivation by a new perturbation method of the high-power describing function of a reactor with linear reactivity feedback mechanisms. Certain previously reported results were shown to be incomplete or incorrect. The new derivation and a computer program for calculating the high-power describing function provides a more accurate, dependable, and convenient tool for analyzing reactor stability in the presence of large amplitude reactivity variations than has previously been available. This paper was based on work recently published in an AEC report [10].

(f) "Failure of Spert III Pressurizer Vessel", by R. E. Heffner, Trans. Am. Nuclear Soc., 5, 1, p 135 (1962).

This paper described the failure of the Spert III pressurizer vessel and the causes of the failure, and was based on a recently issued report [11].

---

* Oak Ridge National Laboratory

V. REFERENCES

1. Quarterly Technical Report for Spert Project, 1st Qtr 1962, IDO-16788, pp 1-9 (1962).

2. Quarterly Technical Report for Spert Project, 3rd Qtr 1960, IDO-16677, pp 9-11 (1961).

3. Quarterly Technical Report for Spert Project, 4th Qtr 1960, IDO-16687, pp 5-8 (1961).

4. Quarterly Technical Report for Spert Project, 2nd Qtr 1961, IDO-16716, pp 14-18 (1961).

5. Quarterly Technical Report for Spert Project, 3rd Qtr 1961, IDO-16726, pp 12-17 (1961).

6. Quarterly Technical Report for Spert Project, 3rd Qtr 1961, IDO-16726, pp 18-23 (1961).

7. J. E. Meyer, W. D. Peterson, ART-04, A Modification of the ART Program for the Treatment of Reactor Thermal Transients on the IBM 704, WAPD-TM-202 (1960).

8. J. V. Reihing, Jr., W. G. Clark, An Appraisal of the MIM and ART Differencing Methods Employing M0076, A Digital Frequency Analysis Program, WAPD-TM-286 (1961).

9. A. H. Spano et al, Self-Limiting Power Excursion Tests of a Water-Moderated Low Enrichment UO_2 Core in Spert I, IDO-16751 (1962).

10. A. A. Wasserman, Contributions to Two Problems in Space-Independent, Nuclear Reactor Dynamics, IDO-16755 (1962).

11. R. E. Heffner et al, Spert III Pressurizer Vessel Failure, IDO-16743 (1962).

PHILLIPS
PETROLEUM
COMPANY

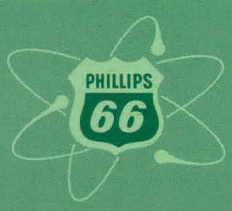

ATOMIC ENERGY DIVISION